Advanced Rate-Based Simulation Tool for Reactive Distillation

E. Y. Kenig and A. Górak
Dept. of Chemical Engineering, Dortmund University, 44221 Dortmund, Germany

A. Pyhälahti
Neste Engineering Oy, Porvoo, Finland

K. Jakobsson and J. Aittamaa
Helsinki University of Technology, Helsinki, Finland

K. Sundmacher
Max-Planck-Institute for Dynamics of Complex Technical Systems, Magdeburg, Germany

A rigorous rate-based modeling approach to reactive distillation equipment is presented in detail. This approach has succeeded from the three-year project "Reactive Distillation" initiated by SUSTECH and supported by the EU in the frame of the BRITE-EURAM program. As a result, a steady-state rate-based simulator DESIGNER has been created and tested with industrially important reactive distillations. First, a thorough description of the model development, including process hydrodynamics and kinetics, is given. The general structure of DESIGNER is highlighted. Furthermore, numerical problems, simulation issues, and validation of the developed simulator are discussed, whereas several industrially important applications are demonstrated. The main advantages of DESIGNER are the direct account of mass and heat transport (rate-based approach), multicomponent mass-transport description via the Maxwell-Stefan equations, consideration of a large spectrum of reactions (homogeneous and heterogeneous; slow, moderate, and fast; equilibrium and kinetically controlled), reaction account in both bulk and film phases, availability of different hydrodynamic models, and a large choice of hydrodynamic and mass-transfer correlations for various types of column internals (trays, random and structured packings, catalytic packings). Particular attention is devoted to the mass-transfer model, including the reaction in the film region, to the catalyst efficiency determination based on the mass transfer inside the catalyst and to the hydrodynamic models for reactive trays. © 2004 American Institute of Chemical Engineers *AIChE J,* 50: 322–342, 2004

Keywords: reactive distillation, rate-based approach, film reactor, reactive tray hydrodynamics, Maxwell-Stefan equations, methyl acetate, MTBE

Introduction

Many traditional processes related to the chemical industries comprise different stages: reaction and separation. These operations are carried out in distinct equipment units, and thus equipment and energy costs are determined from these major steps.

In the past two decades there has been a permanently increasing interest in the development of hybrid processes combining reaction and separation mechanisms into a single, simultaneous operation. Such combined processes are called reactive separation processes. The combination of the reaction and separation stages into a single unit gives rise to several important advantages, among which are energy and capital cost

Correspondence concerning this paper should be addressed to E. Y. Kenig at e.kenig@bci.uni-dortmund.de.

reduction, increase of reaction yield, and overcoming thermodynamic restrictions such as azeotropes (DeGarmo et al., 1992; Doherty and Buzad, 1992; Malone and Doherty, 2000).

By far the most important representative of reactive separation processes is *reactive distillation,* whereby reaction and separation take place within a single countercurrent column. Reactants are converted to products in a reaction zone with simultaneous separation of the products and recycle of unused reactants to the reaction zone. Among suitable reactive distillation processes are etherifications, nitrations, esterifications, transesterifications, polycondensations, alcylations, and halogenations. The reactive distillation process is both efficient in size and cost of capital equipment and in the energy used to achieve a complete conversion of reactants. The process is more intensive and at the same time cleaner because fewer waste products are produced. Since reactor costs are often less than 10% of the capital investment, the combination of a relatively cheap reactor with a distillation column offers great potential for overall savings. Several reviews have been published in the last decade that give an excellent introduction to and overview of reactive distillation processes (see Doherty and Buzad, 1992; Taylor and Krishna, 2000; Sakuth et al., 2001; Towler and Frey, 2001; Wörz and Mayer, 2001; Noeres et al., 2003).

The applicability of reactive distillation is related to the chemical system at hand. Cases where reactive distillation is advantageous are those where azeotropes can be avoided in the separation part of the process, increasing the conversion or selectivity of the reaction or those where closely boiling mixtures should be separated. The most obvious candidates for reactive distillation application are systems with unfavorable reaction equilibrium and significant heat of reaction, where feasible distillation and reaction temperature ranges overlap (see Doherty and Buzad (1992) for more details).

Optimal performance of reactive distillation operations depends largely on a relevant process design, properly selected column internals, feed locations, catalyst choice, as well as on sufficient understanding of general and particular features of the process behavior. All this unavoidably necessitates application of well-working, reliable, and adequate process models.

Under the initiative of SUSTECH, the consortium of the companies BP Chemicals (Great Britain), Hoechst (Germany), BASF (Germany), Snamprogetti (Italy), Neste Oy (Finland), and the Universities of Clausthal (Germany), Dortmund (Germany), Aston (Great Britain), Bath (Great Britain), and Helsinki University of Technology (Finland) took hold of the challenge of modeling reactive distillation processes. In the course of the large-scale three-year BRITE-EURAM project, the process models have been created and integrated with the solver and data bases to form a completely rate-based steady-state simulator called *DESIGNER,* which has been tested against industrially important reactive distillations (see Kenig et al., 1999).

In the present article we give a detailed description of the modeling approach developed and used in the project just cited. First, a general column description and the rate-based stage modeling are discussed. Further, we concentrate on the aspects of particular interest for the DESIGNER development that are the mass-transfer model, including the reaction in the film region, the catalyst efficiency determination based on the mass transfer inside of the catalyst, and the hydrodynamic models for reactive trays. Afterwards, the general structure of DESIGNER is presented and a number of numerical problems, simulation examples, and validation aspects are highlighted.

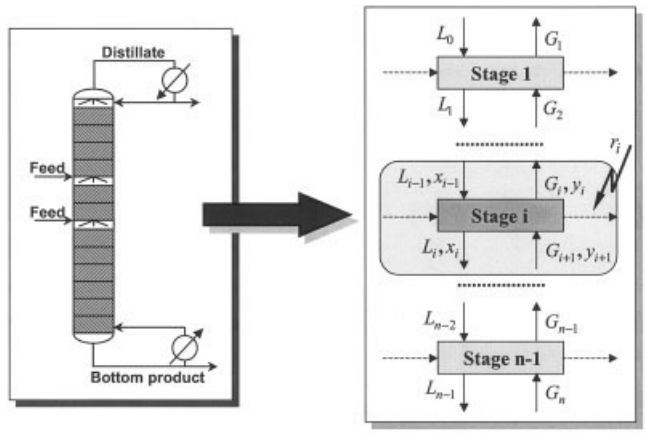

Figure 1. Discretization of a reactive distillation column.

Column Model

One can distinguish between two types of reactive distillation. The first one is the homogeneously catalyzed reactive distillation, with a liquid catalyst acting as a mixture component. Homogeneously catalyzed reactive distillation presents essentially a combination of transport phenomena and reactions taking place in a two-phase system with an interface. The second type is the heterogeneously catalyzed reactive distillation or the so-called catalytic distillation, where the reaction takes place inside a solid catalytic phase. Both types have their advantages, which are detailed elsewhere (see, for example, Agreda et al., 1990; Doherty and Buzad, 1992; Sundmacher et al., 1994).

Both homogeneously and heterogeneously catalyzed reactive distillations are of a multicomponent nature. This means that they are qualitatively more complex than similar binary processes. Thermodynamic and diffusional coupling at the interface and in the phases that are of multicomponent character (Taylor and Krishna, 1993; Kenig and Górak, 1995) are accompanied by complex chemical reactions. As a consequence, to describe such processes adequately, we need specially developed mathematical models capable of taking into consideration column hydrodynamics, mass-transfer resistances, and reaction kinetics.

In DESIGNER, both homogeneously and heterogeneously catalyzed reactive distillations are tackled using a single column model representation. The model of the reactive distillation unit is based on the discretization of the column (Figure 1). The discretization elements (the so-called *stages*) are identified with real trays, for example, of a sieve tray column, or the segments of a packed column. They can be described by various theoretical concepts. Most of the reactive distillations have been designed based on the *equilibrium stage model* (Henley and Seader, 1981) completed with the equations for chemical reaction equilibrium. However, such a rough approach is only valid for very fast reactions and can hardly give the required modeling accuracy. This is due to the fact that

reactive distillation is mostly kinetically controlled by chemical reactions as well as by mass-transport phenomena.

In our project we have chosen a more progressive and physically consistent way that permits a direct account of process kinetics. This approach to the description of a column stage is known as *the rate-based approach* (Seader, 1989; Katti, 1995) and implies that actual rates of multicomponent mass transport, heat transport, and chemical reactions are taken into account directly.

Mass transfer at the vapor–liquid interface is described via the two-film model (Lewis and Whitman, 1924). In this model, it is assumed that all of the resistance to mass transfer is concentrated in thin films adjacent to the vapor–liquid interface and that transfer occurs within these films by steady-state molecular diffusion alone. Outside the films the level of mixing is so high that no composition gradients exist in the bulk fluid phases at all. This means that in the film region we have one-dimensional diffusional transport normal to the interface.

Multicomponent diffusion in the films is described by the Maxwell-Stefan equations, which can be derived from the kinetic theory of gases (Hirschfelder et al., 1964). The Maxwell-Stefan equations connect the diffusion fluxes of the components with the gradients of their chemical potential. With some modifications these equations can be recast into a generalized form in which they are often used for the description of real gases and liquids (Taylor and Krishna, 1993)

$$\frac{x_i}{R_m T}\frac{d\mu_i}{dz} = \sum_{j=1}^{n}\frac{x_i N_j - x_j N_i}{c_t \mathcal{D}_{ij}}; \quad i = 1, \ldots, n. \tag{1}$$

Thus the vapor–liquid mass transfer is modeled based on the film theory using the Maxwell-Stefan approach to express the fluxes in the multicomponent mixture as functions of the driving forces, that is, the concentration differences across the films. In this stage model approach, the equilibrium state exists only at the interface. The relevant thermodynamic equations connecting the interfacial values of concentrations and temperature play an important part in the calculation of the stage characteristics (see below).

The hydrodynamic effects are taken into account by applying correlations for mass-transfer coefficients for the liquid and vapor phases, specific contact area, liquid holdups, pressure drop, weeping, and entrainment. On the stage scale there are several hydrodynamic models available. In DESIGNER these models are collected in a special model library containing hydrodynamic and mass-transfer correlations for a number of different column internals and flow conditions.

For large cross-flow trays, some new ideas of modeling the effects of concentration gradients in the liquid phase have been developed. These ideas are based on the mixed-pool model and the eddy diffusion model (see the section titled "Modeling of Reactive Trays Hydrodynamics").

The reaction influences concentration (and temperature) profiles on the stage, and this changes the process behavior. The reaction models developed in the project are divided into three types:

- Effective kinetic models;
- Homogeneously catalyzed reaction models, including reaction in the liquid film;
- Heterogeneously catalyzed reaction models based on the catalyst effectiveness-factor concept.

The effective kinetic model represents the description of the kinetic mechanisms introduced as source terms into the balance equations of the reactive distillation column. In the homogeneously catalyzed reaction model, the film reaction mechanism is added in which the governing mass-transfer equation includes a matrix diffusion term (described by the Maxwell-Stefan equations) and a reaction term (Kenig et al., 1992; Kenig and Górak, 1995). The heterogeneously catalyzed model is based on a generalization of the catalyst model as proposed by Sundmacher and Hoffmann (1996). The two latter kinetic models are presented in detail in the sections titled "Film Phenomena in Homogeneously Catalyzed Reactive Distillation" and "Reaction and Mass Transfer in Macroporous Catalyst."

The column model of DESIGNER comprises several modifications that have their own set of independent variables and equations and, in some cases, even their own solution method. Basically, the column models can be classified as follows:

- Completely mixed liquid–completely mixed vapor;
- Completely mixed liquid–vapor plug flow;
- Mixed-pool model;
- Eddy-diffusion model based on analytical solution of the linearized eddy-diffusion equations;
- Eddy-diffusion model based on rigorous numerical solution of the eddy-diffusion equations.

The first two models follow established theories (see, for example, Toor, 1964b; Taylor and Krishna, 1993; Kooijman and Taylor, 1995). The rate-based mixed pool model and the eddy diffusion models for reactive distillation are new developments of this project.

The reboiler and condenser of the column are modeled as nonreactive equilibrium stages. The implementation allows that all individual stages can be specified separately and independently. In addition, if relevant, a stage design defined for one stage can be copied to describe other similar stages.

Rate-Based Stage Modeling

Balance equations

The mass-balance equations of the traditional multicomponent rate-based model (see, for example, Taylor and Krishna, 1993; Kenig and Górak, 1995) are written separately for each phase. During the reactive distillation, chemical reactions take place in the liquid phase, therefore, the liquid-phase balances should be modified in order to include the reaction source terms

$$0 = -\frac{d}{dl_a}(L x_i^B) + (N_{Li}^B a^I + R_{Li}^B \phi_L) A_c; \quad i = 1, \ldots, n \tag{2}$$

$$0 = \frac{d}{dl_a}(G y_i^B) - N_{Gi}^B a^I A_c; \quad i = 1, \ldots, n. \tag{3}$$

In Eqs. 2 and 3, it is assumed that transfers from the vapor to the liquid phase are positive.

The bulk-phase balances are completed by the summation equation for the liquid and vapor bulk mole fractions, respectively

$$\sum_{i=1}^{n} x_i^B = 1 \tag{4}$$

$$\sum_{i=1}^{n} y_i^B = 1. \tag{5}$$

The volumetric liquid holdup ϕ_L depends on the vapor and liquid flows and is calculated from empirical correlations (Mackowiak, 1991; Rocha et al., 1993). The gas holdup has been neglected due to the low operating pressure of the column.

The energy-balance equations of the traditional multicomponent rate-based model (cf. Taylor and Krishna, 1993) are applied here

$$0 = -\frac{d}{dl_a}(Lh^B) + Q_L^B a^I A_c \tag{6}$$

$$0 = \frac{d}{dl_a}(GH^B) - Q_G^B a^I A_c. \tag{7}$$

We adopted the convention of using the heat of formation of the components as the reference state for enthalpy calculations. Thus the heat of reaction is considered in the balances (Eqs. 6 and 7) implicitly, without using an explicit source term.

Mass transfer and reaction in the film

The vapor-phase film mass transport is described by the following conservation equation

$$\frac{dN_{Gi}^f}{dz_f} = 0, \quad i = 1, \ldots, n. \tag{8}$$

The liquid film is considered as an additional region in which reaction and mass transfer occur simultaneously

$$\frac{dN_{Li}^f}{dz_f} - R_{Li}^f = 0, \quad i = 1, \ldots, n. \tag{9}$$

Due to the chemical conversion in the liquid film, the molar fluxes at the interface, N_i^I, and at the boundary between the film and the liquid bulk phase, N_{Li}^B, differ. The system of equations is completed by the energy-conservation equations in both films, by the conservation equations for the mass and energy fluxes at the phase interface and by the necessary linking conditions between the bulk and film phases (see Taylor and Krishna, 1993).

The film thickness is an important model parameter that is usually estimated via empirical mass-transfer coefficient correlations allowing for the influence of column internals, hydraulics, and transport properties (Górak, 1995). In the project, the most suitable and reliable correlations for a number of structured and random packings and trays have been chosen from the open literature, thoroughly tested, and implemented into DESIGNER.

A special consideration has been devoted to the case of catalytic distillation, where heterogeneous reactions occur in the liquid phase (see the section titled "Reaction and Mass Transfer in Macroporous Catalyst").

Hydrodynamics

The rate-based modeling of the reactive distillation column requires information on hydrodynamic variables, as, for example, liquid holdup. These values are determined and presented as certain correlations depending on a number of hydrodynamic, geometric, physicochemical quantities such as Reynolds number, Schmidt number, and equivalent column diameter. There are numerous studies devoted to the description of hydrodynamic behavior of packed and tray columns basing on empirical correlations within certain limited ranges of operating conditions (see, for example, Sherwood et al., 1975; King, 1980; Treybal, 1980; Zogg, 1983; Lockett, 1986; Kister, 1992).

In this project, a large number of open literature correlations describing the hydrodynamic properties of both tray and packed columns is considered and implemented into DESIGNER.

Recent structured packing models for pressure drop and liquid holdup usually use the concepts of the *channel model* or *particle model* (see Stichlmair et al., 1989; Rocha et al., 1993). In the channel model, the vapor is assumed to flow upward inside numerous small channels having some characteristic dimensions. The liquid flows down the channel walls, reducing the available cross-sectional area for vapor flow. In the particle model, an analogy between a vapor–liquid contacting device and a fluidized bed is utilized by defining an effective bed porosity that changes with geometry and liquid holdup.

The total holdup is the sum of the dynamic and static holdup. The static holdup is the stagnant liquid prevailing in pores and gaps of the packing. The dynamic holdup is the volume of liquid flowing down the packing. From experimental investigations it follows that in the preloading regime the volume of the liquid holdup on the packing depends on the kind and size of packing (the static holdup), the physical properties of the liquid, and the liquid flow velocity. After exceeding a certain flow rate, the friction between gas and liquid phases becomes significant and the liquid holdup depends also on the gas flow rate (loading range).

Pressure-drop correlations consist of two parts. The first part is the pressure drop for a dry column, which is a function of the packing size, gas velocity, and physical properties of gas. The second part is the pressure drop for a wet column, which additionally depends on the liquid flow rate and physical properties of the liquid.

For the tray columns, pressure drop, liquid holdup, entrainment, and weeping are the usual hydrodynamic variables to be taken into account. An extensive set of correlations for these variables is included in the model library. Eddy diffusivity has been usually less frequently dealt with, but it is important when the concentration profiles over an individual plate are considered, and, hence, the correlations for the eddy diffusivity are included as well.

In this project, special attention has been devoted to the cross-flow tray modeling (see the section titled "Modeling of Reactive Trays Hydrodynamics").

Chemical reactions

Reactions considered in the project are of two different types: homogeneous reactions in homogeneously catalyzed reactive distillation, and heterogeneous reactions in catalytic distillation. Independently of the reaction location, character, and rate, its modeling is closely related to the column-stage representation, as described earlier. This gives us an opportunity to incorporate the reaction models directly, as rate terms, into the set of independent variables and equations developed for separation problems.

In the project, an extensive experimental program has been performed in order to investigate industrially important reactive systems (homogeneously and heterogeneously catalyzed esterifications, etherifications, alkylations) and to develop kinetic models for these reactions.

Physical properties and thermodynamics description

A large number of necessary physical properties are computed with standard methods. DESIGNER can use different physical property packages that are easy to interchange. One of these packages is *the thermodynamic interface IK-CAPE* developed in a cooperative project involving most large German chemical companies (Fieg et al., 1995). In the project, some partners used their own thermodynamic programs implemented into their in-house databanks.

The determination of the Maxwell-Stefan diffusivities is based on diffusion coefficients at infinite dilution. In DESIGNER different methods available in the open literature (see Taylor and Krishna (1993); Wesselingh and Krishna (2000)) are implemented.

At the vapor–liquid interface, the thermodynamic equilibrium between the two phases is assumed

$$y_i^I = K_i x_i^I, \quad i = 1, \ldots, n. \tag{10}$$

The distribution coefficient, K_i, comprises fugacities in both phases and activity coefficients in the liquid phase. They can be calculated by different methods (see, for example, Reid et al. (1987)).

Film Phenomena in Homogeneously Catalyzed Reactive Distillation

In this project, a kinetic description of the stage that takes the reaction mechanism into account has been developed. A widely used approximation that reactions influence the mass- and heat-transfer rates without changing the liquid-film thickness has been exploited (Danckwerts, 1970; Doraiswamy and Sharma, 1984; Kenig and Górak, 1995). The latter can thus be determined from binary correlations obtained experimentally or theoretically for a given mode of phase contact (Kenig and Górak, 1995). The stage models involving the reaction consideration in the film are thought to be realized as separate procedures intended to calculate the values of mass fluxes, which are then implemented into the balance equations of the model.

Governing equations

Homogeneous reactions result in the reaction volume source (the rate of producing of reacting species per volume of a mixture). The relevant reaction term depends on the mixture composition and temperature. Our task is to account for this source, first, in the bulk liquid and, second, inside of the liquid film. The latter influences and changes the values of molar fluxes.

Considering diffusional mass transfer in the film and using vectorial form, Eq. 9 transforms to

$$-\frac{d\tilde{\mathbf{J}}_L}{d\xi}\cdot\frac{1}{\delta_L}+\tilde{\mathbf{R}}=0, \tag{11}$$

where the dimensionless film coordinate ξ is defined as

$$\xi=\frac{z_f}{\delta_L}. \tag{12}$$

The following boundary conditions for Eq. 11 are specified by the film model

$$\mathbf{x}(\xi=0)=\mathbf{x}^I, \quad \mathbf{x}(\xi=1)=\mathbf{x}^B \tag{13}$$

In terms of the concentration vector, Eq. 11 is a nonlinear differential equation of the second order. Therefore, the boundary-value problem (Eqs. 11 and 13) has to be solved numerically. However, this numerical solution may cause significant calculation difficulties associated with convergence and stability of numerical procedures, which can be of a particular relevance when industrial reactive separation units are considered and designed.

To avoid numerical technique we suggest another approach that is based, first, on the *linearized theory of multicomponent diffusion* suggested by Toor (1964a) and Stewart and Prober (1964), and, second, on a linear approximation of the reaction term suggested by Wei and Prater (1962)

$$\mathbf{R}\cong-[K]\mathbf{x}. \tag{14}$$

Equation 14 represents one of the best approaches to the modeling of complex reaction systems and provides a satisfactory representation for many rate processes over the entire range of reactions, as well as linear approximations for most systems in a sufficiently small range (see, for example, Hikita and Asai (1964); Toor (1965); DeLancey (1974); Doraiswamy and Sharma (1984)). Equation 14 has gained widespread acceptance in various chemical and reactor engineering areas (Astarita and Sandler (1991) and is recommended for use in the modeling of reactive separation operations (DeLancey, 1974; Kenig et al., 2000).

With these approximations, Eq. 11 turns to the following one (Kenig and Górak, 1995)

$$[D]\frac{d^2\mathbf{x}}{d\xi^2}=\delta_L^2[K]\mathbf{x} \tag{15}$$

Matrix $[D]$ results from the transformation of the Maxwell-Stefan equations (Eqs. 1) to the form of the generalized Fick's law (Toor, 1964a). Matrix $[D]$ is generally a function of the mixture composition and is assumed constant along the diffu-

sion path (Toor, 1964a; Stewart and Prober, 1964). The direct expressions for the elements of the diffusion matrix $[D]$ can be found, for example, in Taylor and Krishna (1993).

From the modeling point of view, the use of the linearized kinetics means that a loss in accuracy on the stage of model formulation is compensated during the solution. If the linearization is accomplished with reasonable exactness, such approximation seems to be good enough for getting adequate results, and we can thus avoid calculation trouble.

Solution

The solution to the linearized problem (Eqs. 11 and 13) is obtained analytically using matrix algebra operations (see Kenig and Górak, 1995)

$$\mathbf{x} = \sinh\{[\Psi]\delta_L(1-\xi)\}\sinh^{-1}\{[\Psi]\delta_L\}\mathbf{x}^I - \sinh\{-[\Psi]\delta_L\xi\}\sinh^{-1}\{[\Psi]\delta_L\}\mathbf{x}^B, \quad (16)$$

where

$$[\Psi] = ([D]^{-1}[K])^{0.5}. \quad (17)$$

Differentiating Eq. 16 and substituting $\xi = 1$ gives the molar fluxes into/from the bulk of the liquid phase

$$\mathbf{J}_L\big|_{\xi=1} = c_L[D][\Psi]\{\sinh^{-1}([\Psi]\delta_L)\mathbf{x}^I - \coth([\Psi]\delta_L)\mathbf{x}^B\}, \quad (18)$$

whereas the same operation at $\xi = 0$ allows the interface fluxes to be obtained:

$$\mathbf{J}_L\big|_{\xi=0} = c_L[D][\Psi]\{\coth([\Psi]\delta_L)\mathbf{x}^I - \sinh^{-1}([\Psi]\delta_L)\mathbf{x}^B\}. \quad (19)$$

Equations 18 and 19 thus define simple expressions for the component fluxes with due regard to the homogeneous reaction in the liquid film.

Case when all components react

In this case, the differential equation describing the film-region phenomena differs from Eq. 15 (see Kenig and Kholpanov, 1992) and takes the form

$$[D]\frac{d^2\mathbf{x}}{d\xi^2} = \delta_L^2([\hat{K}]\mathbf{x} + \mathbf{a}), \quad (20)$$

where

$$[\hat{K}]_{ij} = [\tilde{K}]_{ij} - [\tilde{K}]_{in}, \quad a_i = [\tilde{K}]_{in}, \quad i,j = 1,2,\ldots,n-1 \quad (21)$$

The solution of the problem (Eqs. 18 and 19) is as follows:

$$\mathbf{x} = \mathbf{x}_H + \sinh\{[\Psi]\delta_L(1-\xi)\}\sinh^{-1}\{[\Psi]\delta_L\}(\mathbf{x}^I - \mathbf{x}_H) - \sinh\{-[\Psi]\delta_L\xi\}\sinh^{-1}\{[\Psi]\delta_L\}(\mathbf{x}^B - \mathbf{x}_H) \quad (22)$$

where vector $\mathbf{x}_H$ is defined by (see Kenig and Kholpanov, 1992)

$$\mathbf{x}_H = -[\hat{K}]^{-1}\mathbf{a} \quad (23)$$

The expressions for the molar fluxes (Eqs. 18 and 19) are obtained similarly to the case considered earlier.

If a single reaction is considered, with all components taking part in it (for example, esterification), the matrices $[\tilde{K}]$ and $[\hat{K}]$ become singular. For this case, a special technique has been worked out to calculate the vector $\mathbf{x}_H$.

Determination of the reaction matrix

Usually the kinetics of chemical reactions are not of the first order. In a multicomponent mixture, which appears in homogeneous reactive distillation, the reaction kinetics is normally described by a product of powers of the reactant concentrations (the mass action law) (Danckwerts, 1970). As a first approximation, the reaction orders can be set to the stoichiometric coefficients in the reaction. Just in exceptional cases, when the reaction is of the first order, the kinetic expression can be implemented into the differential equations resulting in analytically solvable boundary-value problems. Otherwise, the reaction kinetics have to be linearized in such a way that the errors between the real and linearized kinetics are minimal.

The mathematical expression corresponding to the mass-action law is as follows

$$r = k_{for}\prod_{j=1}^{n} c_j^{m_j} - k_{rev}\prod_{j=1}^{n} c_j^{m_j} \quad (24)$$

where k_{for} and k_{rev} are temperature-dependent rate constants of the forward and reverse reaction. Equation 24 is first subdivided into the forward and reverse reaction, and then each part is linearized by the least-square method. DeLancey (1974) suggested the following criterion for the linearization

$$\operatorname*{Min}_{k_j}\int_{c_{1B}}^{c_{1I}}\int_{c_{2B}}^{c_{2I}}\cdots\int_{c_{nB}}^{c_{nI}}\left[k_{for/rev}\prod_{i=1}^{n} c_i^{m_i} - \sum_{\substack{j=1\\ m_j\neq 0}}^{n} k_j c_j\right]^2 dc_1 dc_2,\ldots,dc_n. \quad (25)$$

By this criterion the constants k_j, $j = 1, 2, \ldots, n$, are determined for each reaction. To get the minimum of the function in Eq. 25, the integrands are differentiated with respect to all constants k_j, and afterwards they are integrated over the whole concentration simplex (see DeLancey, 1974; Kenig et al., 2000).

The integration results in a standard system of linear algebraic equations, which can be written as

$$\tilde{\mathbf{p}} = [\tilde{Q}]\tilde{\mathbf{k}}. \quad (26)$$

By solving the system (Eq. 26), the linearization constants k_j, $j = 1, 2, \ldots, n$, can be obtained for each reaction.

In DeLancey (1974) a closed solution of the system (Eq. 26) was derived. Unfortunately, this solution cannot be used in its final form because of several errors. We solve the system (Eq. 26) in a different way, by simple inversion of matrix $[\tilde{Q}]$

$$\tilde{\mathbf{k}} = [\tilde{Q}]^{-1}\tilde{\mathbf{p}}. \tag{27}$$

The suggested method is advantageous, since it takes into account the whole concentration simplex.

The vector $\tilde{\mathbf{k}}$ contains the linearization constants, and it is used to obtain the reaction kinetic matrix $[\tilde{K}]$. Multiplying with the stoichiometric coefficients yields

$$[\tilde{K}] = -\begin{pmatrix}\nu_1\\ \nu_2\\ \nu_n\end{pmatrix}\tilde{\mathbf{k}}^T = -\begin{pmatrix}\nu_1\\ \nu_2\\ \nu_n\end{pmatrix}(k_1, k_2, \ldots, k_n). \tag{28}$$

The same approach can be used for the general case, when several reactions occur (cf. Kenig et al., 2000).

The transformation of the matrix $[\tilde{K}]$ (Eq. 28) to the reaction matrix $[K]$ with the dimension $(n - 1)$ is detailed in Kenig and Kholpanov (1992), where the two types of reacting mixtures (with and without chemically inert components) are discriminated. For both types, the analytical formulas such as Eqs. 18 and 19 enable direct estimation of the component molar fluxes.

Validation of the linearization method

Generally, the vector $\tilde{\mathbf{k}}$ (Eq. 27) should be calculated for each reaction using the method just described, for certain specified boundary compositions (which are delivered from an external numerical procedure available in DESIGNER). To test the linearization method, real reaction-rate values have to be compared with the linearized reaction-rate values calculated by

$$r_{lin} = k_1 \cdot c_1 + k_2 \cdot c_2 + \cdots + k_n c_n \equiv k_1' \cdot x_1 + k_2' + \cdots + k_n' x_n, \tag{29}$$

where $k_i' = c_t \cdot k_i$, $i = 1, 2, \ldots, n$.

The comparison can be accomplished using a variation of one of the mole fractions. The results of the comparison can be seen well when presented as dependencies of the reaction rate on the varied mole fraction, x_j. In Kenig et al. (2000), four examples are demonstrated. The first two examples deal with the esterification of acetic acid by ethanol, with the mass-action law kinetics.

The second two examples treat a more complex kinetic expression of the Langmuir-Hinshelwood type, for the production of MTBE (methyl-*tert*-butyl-ether) from methanol and isobutene (Rehfinger and Hoffmann, 1990a). This formal application is done to make a harder test of the linearization. For systems that do not strictly follow simple power law kinetics, like the MTBE-synthesis, small ranges of mole fraction cause sufficiently small errors. For a wider range, the relative error grows. This cannot be considered to be a disadvantage of the linearization technique, however, since the composition variations in the rate-based simulations are related to a single stage rather than to the whole apparatus, and consequently, a rather small mole-fraction difference is expected to be used during the linearization.

For systems that follow mass-action law in a strict sense, still better results are obtained. The relative error in this example is small everywhere, even if the mole fraction varies in a wide range. Thus, the suggested linearization method provides reliable results that can be applied in reactive separation modeling with a reasonable accuracy.

Further testing has been done in Kenig et al. (2000) by comparing the analytical solution based on the linearized Eq. 15 with the numerical solution of Eq. 11 without linearization of the reaction term. This comparison showed that the two methods are almost equivalent in regard to application, provided that care is taken of being within a proper range of process parameters and variables.

Modeling of Reactive Tray Hydrodynamics

The concentration distribution on a cross-flow tray is not even. The flow pattern of the liquid on the tray influences the mass transfer and reaction rates on a distillation tray. The vapor concentration changes gradually when it rises through the liquid on the tray. The liquid concentration also changes gradually from the inlet to the outlet of the tray. Traditionally this phenomenon has been lumped together with many other factors affecting performance of the tray to a quantity called *stage efficiency*. The latter is necessary in order to improve the modeling based on the equilibrium stage consideration (Henley and Seader, 1981). In the rate-based approach, the notion of the stage efficiency is inappropriate; however, the uneven concentration distribution on the tray should be accounted for. In order to improve the accuracy of the rate-based model, instead of the efficiency calculation, the direct modeling of the tray concentration profiles is accomplished.

The situation becomes more complicated if a reaction takes place on the plates. Usually reaction rates are functions of concentrations and temperatures, and thus a rigorous model should consider their possible variations. This represents a difficult challenge, and there have been only very few attempts to tackle it. Among those, Alejski (1991) presented a mixed-pool model for reactive distillation. However, in his model the mass-transfer modeling applied to the individual pools was based on the traditional equilibrium-stage model and efficiency concept. Recently, Higler et al. (1999) suggested a nonequilibrium cell model for reactive distillation tray columns.

There are several different ways to model concentration distributions at a stage. Vapor and liquid can be considered fully mixed vertically and horizontally. This is the approach for both the traditional equilibrium-stage models and the standard rate-based model (see, for example, Taylor and Krishna, 1993). This approach can be improved by assuming that in the vertical direction the vapor is flowing in a plug flow through the liquid (Kooijman and Taylor, 1995). This is similar to the calculation of the so-called point efficiencies for the equilibrium-stage models. Vertical liquid concentration gradients are usually not considered because of the intense mixing due to the vapor flow through the liquid.

In the horizontal direction on the vapor side, it may be assumed that either vapor is totally mixed before it enters the tray, or that, after being separated from the liquid on the tray

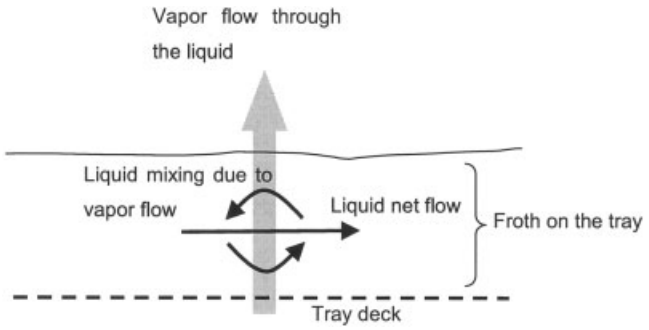

Figure 2. The eddy-diffusion model of a distillation tray.

below, the vapor does not mix at all. The real situation is obviously between these two limiting cases. In small-diameter columns, it is very near to the complete mixing, while in large-diameter columns the vapor is less mixed.

Horizontal liquid flow pattern is very complicated due to the mixing by vapor, dispersion, and the round cross section of the column. On single-pass trays, the latter results in the flow path, which first expands and then contracts. A rigorous modeling of this flow pattern is very difficult, and usually the situation is simplified by assuming that the liquid flow is unidirectional and the major deviation from the plug flow is the turbulent mixing or eddy diffusion.

In DESIGNER, the eddy-diffusion model and the mixed-pool model have been applied in the context of the rate-based reactive distillation model. The plug-flow model for the vapor phase is included as well. However, in the horizontal direction, it is assumed that the vapor phase entering the tray is always completely mixed.

Eddy-diffusion model

The scheme of the plate is presented in Figure 2. Assuming that the flow is one-dimensional, the liquid is completely mixed within the plane perpendicular to the direction of the flow, and the condition of the entering vapor being constant throughout the plate, the basic steady-state eddy-diffusion equations for the components and enthalpy can be written as follows

$$-c_t D_e w h_f \frac{\partial^2 \mathbf{x}(l)}{\partial l^2} - \frac{\partial (L(l)\mathbf{x}(l))}{\partial l} + \mathbf{N}'(l) + \mathbf{R}'(l) = \mathbf{0} \quad (30)$$

$$-c_t D_e w h_f \frac{\partial^2 h(l)}{\partial l^2} - \frac{\partial (L(l)h(l))}{\partial l} + E'(l) = 0. \quad (31)$$

Here $\mathbf{N}'(l)$, $\mathbf{R}'(l)$, and $E'(l)$ are the specific mass transfer rates, reaction rates, and heat-transfer rates per unit length of the tray at distance l from the exit weir, respectively. These terms can be evaluated using the same methods as with the other rate-based models, assuming that the liquid and entering vapor conditions at point l are known (see Taylor and Krishna, 1993; Kenig and Górak, 1995).

The boundary conditions are set by analogy to conditions applied to the nonreactive trays (Gerster et al., 1958)

$$\mathbf{x}\big|_{l=0} = \mathbf{x}_k \quad (32)$$

$$\left.\frac{d\mathbf{x}}{dl}\right|_{l=0} = \mathbf{0}. \quad (33)$$

Similar conditions hold for enthalpy as well. Equation 32 determines the exit concentrations of a tray, whereas Eq. 33 implies that there are no concentration gradients in the liquid near the exit weir. The condition given by Eq. 33 is similar to the one applied by Gerster et al. (1958) to the efficiency calculation of plates for the traditional equilibrium-stage model.

Formally, the eddy-diffusion equation is similar to the corresponding molecular-diffusion equation; however, the eddy diffusivity coefficient depends only on the flow conditions on the tray, and thus is the same for all components. There are several experimental correlations available in the literature that have been implemented in the model library. Their predictions vary considerably. The reaction and mass-transfer terms of Eqs. 32 and 33 are complex nonlinear functions of the compositions, flow rates, and temperatures.

Thus, a numerical solution is the only possibility if a rigorous solution is required. Implementing the numerical solution algorithm is straightforward, but the system of the column equations valid for the standard rate-based model requires significant changes. The reason is that a number of the variables, assuming single values in the completely mixed liquid model, are replaced by continuous functions. It is possible to discretize the differential equation system, to include the discretized equations in the column equation group and solve the whole system simultaneously as an algebraic equation group. However, such a discretization done with sufficient accuracy would result in a very large number of equations to be solved simultaneously, and therefore in DESIGNER a different approach has been selected.

The system of equations describing the column is written as a system of integral equations containing the following items for each tray

- Vapor-side total mass balance

$$0 = -G_k - S_k^G + G_{k-1} - \sum_{i=1}^{n} \left[\int_0^{l_f} N'_{i,k}(l)\, dl \right] + \sum_{i=1}^{n} F_{i,k}^G \quad (34)$$

- Vapor-side component mass balances

$$0 = -(G_k + S_k^G) y_{i,k} + G_{k-1} y_{i,k-1} - \int_0^{l_f} N'_{i,k}(l)\, dl + F_{i,k}^G, \qquad i = 1, \ldots, n \quad (35)$$

- Vapor-side enthalpy balance

$$0 = -(G_k + S_k^G) H_k + G_{k-1} H_{k-1} - \int_0^{l_f} E'_k(l)\, dl + \left(\sum_{i=1}^{N} F_{i,k}^V \right) H_k^F \quad (36)$$

- Liquid-side total mass balance

$$0 = L_{k+1} + \sum_{i=1}^{n} F_{i,k}^L + \sum_{i=1}^{n} \left[\int_0^{l_f} N'_{i,k}(l)\, dl \right] + \sum_{i=1}^{n} \left[\int_0^{l_f} R'_{i,k}(l)\, dl \right] - L_k + S_k^L. \quad (37)$$

- Liquid-side component mass balances

$$0 = L_{k+1}x_{i,k+1} + F^L_{i,k} + \int_0^{l_f} N'_{i,k}(l)\, dl + \int_0^{l_f} R'_{i,k}(l)\, dl - (L_k + S^L_k)x_{i,k}, \quad i = 1, \ldots, n. \quad (38)$$

- Liquid-side enthalpy balance

$$0 = L_{k+1}h_{k+1} + \left(\sum_{i=1}^{n} F^L_{i,k}\right)h^F_k + \int_0^{l_f} E'_k(l)\, dl - (L_k + S^L_k)h_k. \quad (39)$$

- Pressure-drop equation

$$0 = p_k - (p_{k+1} + \Delta p^{spec}_{k+1}) \quad (40)$$

Here index k refers to the tray and index i to the component.

Altogether Eqs. 34–40 represent a system of $2n + 5$ equations instead of the $5n + 6$ equations of the normal rate-based model. Although the number of the equations is considerably reduced, the evaluation of the whole system is still very elaborate.

The integral terms present in the preceding equations are evaluated by solving the systems of differential algebraic equations (DAE) for the plates. This DAE system gives a detailed description of each plate and contains the following equations (the signs of the differentials result from the integration against the flow direction):

- Differential equation for the total liquid flow (eddy diffusion does not produce a net flow)

$$\frac{dL_k}{dl} = -\left(\sum_{i=1}^{n} R'_{i,k} + \sum_{i=1}^{n} N'_{i,k}\right) \quad (41)$$

- Differential equations for the mole fractions of $n - 1$ components in the liquid

$$\frac{d^2x_{i,k}}{dl^2} = -C\left(L_k\frac{dx_{i,k}}{dl} + x_{i,k}\frac{dL_k}{dl} + N'_{i,k} + R'_{i,k}\right), \quad i = 1, \ldots, n-1 \quad (42)$$

- Differential equation for the liquid enthalpy

$$\frac{d^2h_k}{dl^2} = -C\left(h_k\frac{dL_k}{dl} + L\frac{dh_k}{dl} + E'_k\right) \quad (43)$$

- Equation for the sum of the liquid mole fractions

$$0 = 1 - \sum_{i=1}^{n} x_{i,k} \quad (44)$$

- Vapor-side total mass balance

$$0 = G_{k-1} - \left(\sum_{i=1}^{n} N'_{i,k} - G'_k\right)l_f. \quad (45)$$

- Vapor-side enthalpy balance

$$0 = H_{k-1}G_{k-1} - E'_k l_f. \quad (46)$$

- Vapor-side component mass balances

$$0 = y_{i,k-1}G_{k-1} - N'_{i,k}l_f - G'_k y_{i,k}l_f, \quad i = 1, \ldots, n. \quad (47)$$

- Mass-transfer equations

$$0 = N'_{i,k} - N^{calc}_{i,k}, \quad i = 1, \ldots, n. \quad (48)$$

- Equation for the sum of the equilibrium vapor mole fractions

$$0 = 1 - \sum_{i=1}^{n} y^*_{i,k} \quad (49)$$

- Vapor–liquid equilibrium conditions

$$0 = K_{i,k}x_{i,k} - y^*_{i,k}, \quad i = 1, \ldots, n \quad (50)$$

The local heat- and mass-transfer rates per unit length (E' and $\mathbf{N}'$) at the distance l from the liquid outlet edge are calculated using the usual mass-transfer correlations and rate-based vapor plug-flow model, as presented by Taylor et al. (1994). This method is based on the overall mass-transfer coefficient matrix, and thus does not require estimation of the interfacial conditions explicitly, which is advantageous. However, any solution based on the overall vapor-side mass-transfer coefficients requires the composition of the vapor phase at equilibrium with the liquid on the tray, in order to evaluate the mass and energy fluxes (see, for example, Sherwood et al., 1975; Taylor and Krishna, 1993). This is the reason for including Eqs. 49 and 50 in the governing system.

It is worth noting that the principal thermal variable in the DAE system is the liquid enthalpy, rather than the temperature. The main reason is that evaluation of the differential of the enthalpy is much easier than that of the temperature, because the former results directly from the energy balance, whereas the latter is a complex function of system properties.

On the other hand, there is a drawback of this selection, because most thermodynamic property correlations are based on the temperature rather than on the enthalpy, and hence the temperature must be estimated iteratively from the enthalpy, pressure, and composition after the evaluation of the functions has started. However, this penalty is small considering the stability and simplicity of the solution achieved. Therefore, a similar approach has been applied to the solution of the whole system of column equations by the relaxation method (see the section titled "Numerical Solution").

The pressure drop is given as a specification, which is not strictly correct. Nevertheless, this approach is selected because solving the pressure-drop equation rigorously in this context would lead to an overly complicated iteration due to a slight variation in the vapor flux through the tray deck. Moreover, most reactive distillation processes are operated under atmospheric or elevated pressure, and thus the pressure drop is usually not as critical as it would be in vacuum distillation, provided that the column is not hydraulically overloaded. Finally, in practice it is usually easy to generate a reasonably good approximation for the pressure drop by solving the problem with the usual rate-based model and applying the obtained pressure drop as specification for the eddy-diffusion model.

The solution of the main system of equations (Eqs. 34–40) is performed using the block tridiagonal-based Newton method. The evaluation of the integral terms present in Eqs. 34–40 is accomplished by solving the DAE system of equations (Eqs. 41–50) for each tray, starting from the current values of the independent variables at each loop. During the solution of the DAE–equation system, the values of $\mathbf{N}'$, $\mathbf{R}'$,

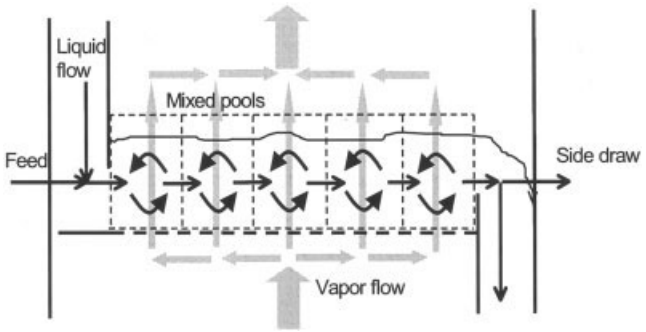

Figure 3. The mixed-pool model of a distillation tray.

and E' are extracted at regular intervals, and the integrals in Eqs. 34–40 are evaluated based on these values.

The DAE-solver used in this case was routine DDRIV3 from the SLATEC Common Mathematical Library, Version 4.1 (see http://www.netlib.org/slatec/index.html).

Mixed-pool model

In this model, the principal idea is that the liquid on the tray is assumed to flow through a series of completely mixed pools. This kind of system can describe approximately the solution of the eddy-diffusion model. It has the advantage that the second-order differential equation group involved in the eddy-diffusion model is replaced by a group of algebraic equations.

The mixed-pool model is somewhat simpler than a similar approach by Higler et al. (1999). The most significant deviation is that the stages are not divided in cells in the vertical direction. There are also some differences in the models implemented and overall structure of the equation group, resulting in a smaller number of independent equations and variables. This can be considered advantageous for a model that is meant for actual design work in which computation time is important.

Figure 3 demonstrates how the tray is divided into the mixed pools. The vapor is assumed to be completely mixed before it enters the tray and to be distributed equally between the segments of the tray.

Each pool has virtually the same variables and equations as the whole tray in the traditional rate-based model. The only deviation is that the pressure is assumed to be constant throughout the plate. Thus, if the number of mixed pools is u and the number of components is n, then there are $5un + 5u + 1$ variables on a tray instead of the $5n + 6$ variables of the traditional rate-based stage. The appropriate number of pools can be determined using the correlations of Ashley and Haselden (1970) and Alejski (1991). The liquid is assumed to be completely mixed in the direction perpendicular to the flow direction.

The independent variables for each tray are:

- u liquid flow rates
- $u \times n$ liquid mole fractions
- $u \times n$ liquid mole fractions at the interface
- u liquid temperatures
- u interfacial temperatures
- $u \times n$ mass-transfer fluxes
- Pressure
- u vapor temperatures
- $u \times n$ vapor mole fractions at the interface
- $u \times n$ vapor mole fractions
- u vapor flow rates.

The corresponding equations to be solved are:

- u liquid-side total mass balances
- $u \times n$ liquid-side component mass balances
- $u \times (n - 1)$ liquid-side mass-transfer equations
- u liquid-side interfacial concentration summation equations
- u liquid-side energy balances
- u interfacial energy balances for each pool
- $u \times n$ interfacial equilibrium equations
- 1 pressure drop condition
- u vapor-side energy balances
- u vapor-side interfacial concentration summation equations
- $u \times (n - 1)$ vapor-side mass-transfer equations
- $u \times n$ vapor-side component mass balances
- u vapor-side total mass balances.

The reboiler and condenser of the column are modeled as equilibrium stages (cf. the section titled "Column Model").

To model the mass transfer in each pool, it is possible to use either the mixed liquid–mixed vapor or the mixed liquid–plug-flow vapor model. The former is based on the approach presented by Taylor and Krishna (1993), whereas the latter model has its origin in Taylor et al. (1994). Both models have been modified by adding the reaction terms to the material balances. In addition, there are two modifications of the latter model, one based on the leaving vapor composition and the second based on the entering composition.

In order to simplify the calculation, the pressure drop is given as a specification similar as it is done for the eddy diffusion model (see earlier). The mixed-pool model is solved using the Thomas algorithm for a block tridiagonal matrix (Patankar, 1980).

Reaction and Mass-Transfer in Macroporous Catalyst

In case of heterogeneously catalyzed reactive distillation, the macropores of the catalyst are filled with the liquid phase of the system. Therefore, the interaction of the internal catalyst mass transport with the microkinetics of the reaction has to be considered. For this purpose, a general mathematical model is developed that allows its application to a number of reaction systems.

Macroporous ion-exchange resin catalysts are commonly used in reactive distillation processes, for example, for etherification and esterification reactions. A new type of such a catalyst, which was also used for the experimental validation of the model developed in the project, are polymer carrier catalysts (Kunz and Hoffmann, 1995). The mass fluxes of the liquid mixture components inside the catalyst are generally influenced by several mechanisms:

- Molecular diffusion in the macropores;
- Viscous flow in the macropores;
- Diffusion along the surface of the gelular phase;
- Diffusion in the gelular phase.

These mechanisms are illustrated by Figure 4. In the present model, it is assumed that mass transport of the components is dominated by the diffusional resistances in the macropores. This has been confirmed by the investigations of Rehfinger and Hoffmann (1990b).

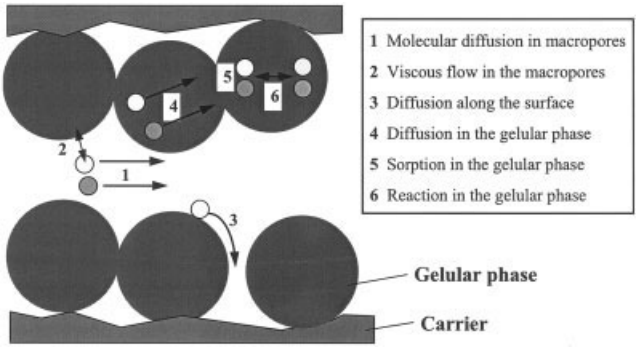

Figure 4. Transport and reaction phenomena inside a polymer–carrier–catalyst.

Model equations

The subsequent formulation of the model equations is similar to that of Sundmacher and Hoffmann (1994). The approach is valid for single chemical reactions at quasi-steady-state conditions. The phenomenon of multicomponent diffusion in pores filled with a nonideal liquid mixture can be described by the generalized Maxwell-Stefan equations (Eq. 1).

At steady-state conditions, the component mass fluxes, N_i, are coupled by the reaction stoichiometry. This yields:

$$\frac{N_i}{\nu_i} = \frac{N_j}{\nu_j} = \ldots = \frac{N_n}{\nu_n} \tag{51}$$

Combining Eqs. 51 with Eq. 1 leads to:

$$N_i = -\frac{c_L}{R_m T}\hat{D}_i \frac{d\mu_i}{dz_p}, \quad i = 1, \ldots, n-1, \tag{52}$$

where

$$\hat{D}_i = \frac{\nu_i x_i}{\sum\limits_{\substack{j=1 \\ j\neq i}}^{n} (x_j\nu_i - x_i\nu_j)/D_{ij}} \tag{53}$$

The mass-transport coefficients $\hat{D}_i$ are taken constant along the diffusion path and are set equal to their values in the liquid bulk phase. The effective mass fluxes are calculated with the relation of Wheeler (1951), taking the catalyst void fraction ε_p and the tortuosity factor τ into consideration:

$$N_{i,eff} = \frac{\varepsilon_p}{\tau} N_i, \quad i = 1, \ldots, n-1 \tag{54}$$

The reaction affinity A_R can be regarded as the driving force for the chemical reaction and is determined as follows:

$$\frac{A_R}{R_m T} = -\ln\left(\frac{1}{K_a}\prod_{i=1}^{n} a_i^{\nu_i}\right) \tag{55}$$

The intrinsic rate equation of a reversible reaction can be formulated by the following power-law kinetics:

$$r = k_{for}(T)\prod_{i=1}^{n} a_i^{m_i}\left(1 - \exp\left[\frac{-A_R}{R_m T}\right]\right). \tag{56}$$

This rate equation can be formulated in terms of the dimensionless reaction affinity α:

$$\alpha = \frac{A_R/R_m T}{(A_R/R_m T)_B} \tag{57}$$

The dimensionless local rate ρ of the chemical reaction within the catalyst particle according to the rate expression Eq. 56 is then given by:

$$\rho(\alpha) = \exp[\lambda(1-\alpha)]\frac{1 - \exp\left]-(A_R/R_m T)_B\alpha\right]}{1 - \exp\left]-(A_R/R_m T)_B\right]} \tag{58}$$

According to this equation, the rate is controlled by the reaction affinity A_R and an enhancement factor λ, which is defined as follows:

$$\lambda \equiv \prod_{i=1}^{n} (m_i\nu_i/\hat{D}_i)\frac{(A_R/R_m T)_B}{MTR} \quad \text{with} \quad MTR \equiv \prod_{i=1}^{n} \nu_i^2/\hat{D}_i. \tag{59}$$

In Eq. 59, the factor MTR stands for the total mass-transfer resistance of the multicomponent mixture in the liquid-filled pores of the catalyst, and m_i represents the reaction order with respect to component i.

Equation 58 is a rate expression in terms of the dimensionless reaction affinity α, and therefore we express the molar flux densities N_i (see Eq. 52) also in terms of α

$$N_i = \nu_i \frac{c_L (A_R/R_m T)^L}{MTR}\frac{d\alpha}{dz_p} \quad i = 1, \ldots, n-1 \tag{60}$$

With Eqs. 58 and 60, the following material balance can be formulated

$$\frac{1}{\zeta^A}\frac{d}{d\zeta}\left(\zeta^A \frac{d\alpha}{d\zeta}\right) = -\phi^2\rho(\alpha) \tag{61}$$

In Eq. 61, A is a catalyst geometry factor ($A = 0$: slab; $A = 1$: cylinder; $A = 2$: sphere). The generalized Thiele modulus ϕ, which appears on the righthand side of the mass balance, is defined by

$$\phi^2 \equiv \left(\frac{L_p^2}{\varepsilon_p/\tau}\right)\frac{r_B MTR}{c_L(A_R/RT)_B} \tag{62}$$

The boundary conditions of the mass balance to be applied are

$$\zeta = 0 \left(\frac{d\alpha}{dz_p}\right) = 0 \tag{63}$$

$$\zeta = 1 \ \alpha = 1. \tag{64}$$

The aim of the presented model is the calculation of the catalyst effectiveness factor η, which is defined by:

$$\eta \equiv (A + 1) \int_0^1 \zeta^A \rho(\zeta) \, d\zeta. \tag{65}$$

The effectiveness factor can be calculated from the solution of the material balance presented by Eq. 61.

According to Sundmacher and Hoffmann (1994), the numerical solution of the given boundary problem (Eqs. 61, 63, and 64) can be obtained by a control-volume discretization of the differential equation. For handling the nonlinear rate expression, Eq. 58, the iteration procedure was slowed down by underrelaxation through artificial inertia.

With the help of Eq. 65, the reaction source term R_i, which appears in the liquid mass balances of a stage, can be expressed as follows:

$$R_i = \nu_i \cdot \eta \cdot r_B, \tag{66}$$

with r_B as the microkinetic rate of reaction at liquid bulk conditions.

Structure of DESIGNER

DESIGNER consists of several major blocks linked together (see Kenig et al., 2001). These blocks include databases, solver and initialization routines, as well as several model libraries. The blocks are related to the specific model constituents, for example, balance relations for the bulk phases, vapor–liquid equilibrium, mass-transfer and hydrodynamic correlations, and reaction equilibrium and kinetics. A detailed description of these model constituents was given above. The libraries involve a number of subroutines coded in Fortran, and a user can easily select a particular subroutine from a library, in accordance with the problem considered. The choice is accomplished with the help of switch facilities described in the DESIGNER manual.

Numerical Solution

DESIGNER comprises a variety of hydrodynamic models presented in the sections titled "Column Model" and "Modeling of Reactive Trays Hydrodynamics").

Regarding the method of solution, these models are broken down into two categories. The models based on completely mixed liquid and completely mixed or plug-flow vapor use well-known developments. Independent variables and equations for these models are similar to those presented by Taylor and Krishna (1993). The equations are slightly modified to include the reaction rates as source terms in the mass balances.

When the film reaction model is applied, it replaces the mass-transfer model. The catalyst efficiency model uses the liquid bulk variables as input, and the model is solved inside the general iteration algorithm. The enthalpies are calculated using the heat of formation as the reference state; therefore, no additional terms for heat of reaction in the enthalpy balances are necessary.

The mass and energy balances and pressure-drop equations are scaled either by preset numbers, or consequently, by total feed flow, total enthalpy of feed, and the specified pressure. The user can choose between different scaling methods.

Another category of hydrodynamic models comprises the eddy-diffusion model and the mixed-pool model. These models have their own numerical solution methods. However, the mixed-pool models can use the solution of the more traditional rate-based models as the starting point.

The numerical solution discussed below is related to the two hydrodynamic models from the first category.

Newton's method

Equations 2 to 10 constitute the basis of the equation set to be solved. This set is completed by the mass- and energy-conservation equations in the films, mass- and heat-transfer correlations, summation equations, reaction kinetics, and so forth. The balance equations are discretized, and we arrive at a large nonlinear algebraic system. The way it is done in DESIGNER is similar to that suggested in (Taylor and Krishna, 1993).

First the highly nonlinear set of the governing equations was solved with Newton's method whereby the new values of the variables were obtained by the following relation

$$\mathbf{X}_{m+1} = \mathbf{X}_m - s\Delta\mathbf{X}_{m+1}, \tag{67}$$

where $\mathbf{X}_m$ is the vector of independent variables of a reactive distillation stage, $\Delta\mathbf{X}_{m+1}$ is the vector of corrections to independent variables, s is a damping factor

$$\mathbf{X}_m = [X_1, X_2, \ldots, X_n]^T,$$

$$\Delta\mathbf{X}_{m+1} = [\Delta X_1, \Delta X_2, \ldots, \Delta X_n]^T.$$

The corrections to the variables are obtained by solving the following linear equation:

$$[J_m]\Delta\mathbf{X}_{m+1} = \mathbf{f}_m \tag{68}$$

where $[J_m]$ is the Jacobian matrix, $\mathbf{f}_m$ is the vector of the residual functions of the stage model $\mathbf{f}_m = [f_1, f_2, \ldots, f_n]^T$.

The Jacobian matrix has a block-tridiagonal structure, which permits a solution of the linearized subset of the equations by the Thomas algorithm (Patankar, 1980). Basically, the computation of the blocks of the Jacobian matrix is performed numerically, with some analytically solved parts of the off-diagonal blocks. The estimation of the step length in the Newton iteration is done either by a quadratic interpolation or by accepting only a step size that reduces the norm of residuals. The user is able to choose between these two damping methods.

The correction of the independent variables is additionally regulated by the existing limits for the process variables. For instance, possible minimum and maximum temperatures and

flow rates can be specified. Values of component concentrations are varied between 0 and 1. It is also possible to define a maximum correction step for the process variables toward their minimum or maximum limits.

Newton's method is fast and robust near the solution; however, its performance strongly depends on the choice of a good initial approximation. The latter represents a general numerical problem.

In our implementation, the initial values for the independent variables can be obtained by using some of the following techniques. The boiling-point compositions and temperature calculated from the averaged feed composition are set as the initial guess of the column compositions and temperatures. The vapor and liquid flows are calculated from a simple mass and energy balances. The rate-based model can also be initialized by solving an ideal stage reactive distillation calculation and extracting the initial values from these results. The ideal stage model is an integrated part of DESIGNER. The initial values can then be given by hand, or the results of a successful simulation can be used to initialize the problem. Considering the fact that the user can specify all calculation methods on each stage, this gives the possibility of applying various combinations of the well-known "homotopy by hand."

Relaxation method

This method usually requires a longer computation time; however, it provides sufficiently better convergence. The application of the relaxation method follows Sundmacher and Hoffmann (1996). The unsteady-state form of the equations is derived by inclusion of accumulation terms in the component mass balances and energy balances.

This treatment of the equations gives a system of DAE for a stage number k in the following form

$$\begin{bmatrix} 0 & & & & & & & & & & \\ & U_k^G & & & & & & & & & \\ & & U_k^G & & & & & & & & \\ & & & 0 & & & & & & & \\ & & & & 0 & & & & & & \\ & & & & & 0 & & & & & \\ & & & & & & 0 & & & & \\ & & & & & & & 0 & & & \\ & & & & & & & & U_k^L & & \\ & & & & & & & & & U_k^L & \\ & & & & & & & & & & 0 \\ & & & & & & & & & & & 0 \end{bmatrix} \frac{d}{dt} \times \begin{bmatrix} G_k \\ \mathbf{y}_k \\ H_k \\ \mathbf{y}_k^I \\ y_{n,k}^I \\ \mathbf{x}_k^I \\ T_k^I \\ L_k \\ \mathbf{x}_k \\ h_k \\ \mathbf{N}_{r,k} \\ N_{r,nk} \end{bmatrix} = \begin{bmatrix} M_{tk}^G \\ \mathbf{M}_k^G \\ E_k^G \\ \mathbf{MT}_k^G \\ S_k^G \\ \mathbf{Q}_k^I \\ E_k^I \\ M_{tk}^L \\ \mathbf{M}_k^L \\ E_k^L \\ \mathbf{MT}_k^L \\ S_k^L \end{bmatrix} \quad (69)$$

Here G_k and L_k are vapor and liquid flow rates, $\mathbf{y}_k$ and $\mathbf{x}_k$ are vapor and liquid bulk composition vectors, H_k^G and H_k^L are vapor and liquid phase enthalpies, $\mathbf{y}_k^I$ and $\mathbf{x}_k^I$ are interfacial vapor and liquid composition vectors, T_k^I is the interfacial temperature, $\mathbf{N}_{r,k}$ is the vector of mass-transfer rates. Further variables in Eq. 69 denote the following equation groups (cf. Taylor and Krishna, 1993): M_{tk}^G and M_{tk}^L total material balances for the vapor and liquid phases; $\mathbf{M}_k^G$ and $\mathbf{M}_k^L$ component material balances for the vapor and liquid phases; E_k^G, E_k^L, and E_k^I energy balances for the vapor and liquid phases and around the interface; $\mathbf{MT}_k^G$ and $\mathbf{MT}_k^L$ mass-transfer rates in the vapor and liquid phases; S_k^G and S_k^L are summation equations for the vapor and liquid phases; and $\mathbf{Q}_k^I$ is equilibrium equations at the interface.

Vectors $\mathbf{y}_k$, $\mathbf{x}_k$, $\mathbf{x}_k^I$, $\mathbf{M}_k^G$, $\mathbf{M}_k^L$, and $\mathbf{Q}_k^I$ are of dimension n, and vectors $\mathbf{y}_k^I$, $\mathbf{MT}_k^G$, $\mathbf{N}_{r,k}$, and $\mathbf{MT}_k^L$ are of dimension $n - 1$. The vapor and liquid inertia terms U_k^G and U_k^L are taken to be constant.

The equations describing the rate mechanisms (kinetics and mass transfer) are treated as constitutive equations, they are introduced into the balance equations as functions of independent variables (concentrations, temperatures, flow rates, and so on).

The obtained DAE-system is solved with the solver LIMEX, which is available from the Konrad Zuse Zentrum (Berlin, Germany, http://www.zib.de/).

Hybrid method

To overcome the initialization problem, a hybrid method was developed that combines both relaxation and Newton's methods. The flow chart of the hybrid method is presented in Figure 5.

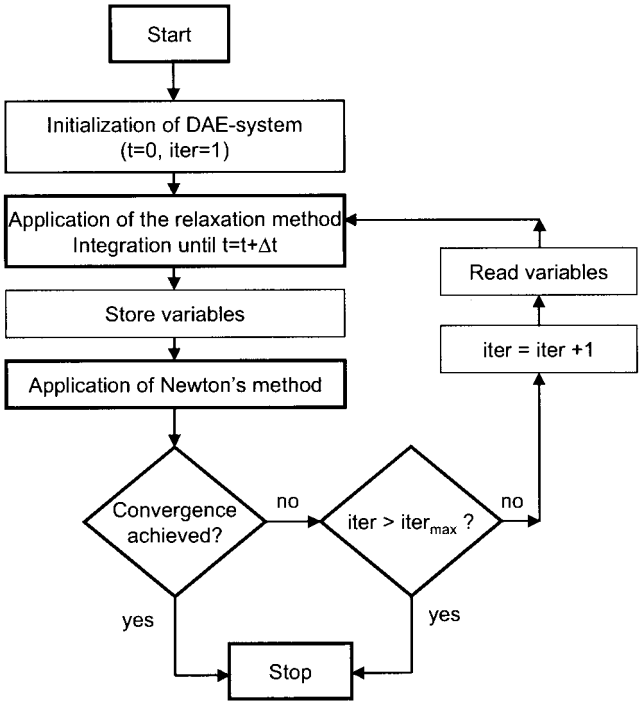

Figure 5. The flow chart of the hybrid algorithm.

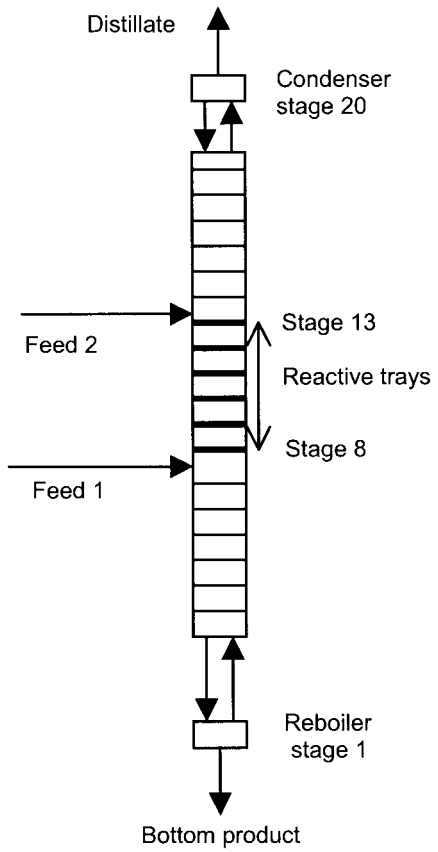

Figure 6. The column used in examples for the eddy-diffusion model and mixed-pool model.

The algorithm starts by the initialization of the DAE system. The requirement is that the algebraic part of the equation system is satisfied. This can be achieved by initializing the bulk liquid compositions, $\mathbf{x}^B$, and interfacial compositions, $\mathbf{x}^I$, by the average feed liquid compositions, setting the vapor compositions $\mathbf{y}^B$, $\mathbf{y}^I$, and the temperatures T^L, T^I, T^G to the bubble-point conditions. The mass-transfer rates are set to zero and the reaction rates are computed at this condition. Finally, the total mass and energy balances for each stage of the column are solved to yield the liquid and vapor flow rates.

It is worthy of note that, from time to time, this initialization procedure fails to give a good starting point for the integration, and the flow values become negative. For this reason, another way to initialize the variables was developed, by which a user can specify the stage liquid compositions directly instead of applying the average feed compositions as described earlier. In this case, the reaction rates are first set to zero. During the integration they are recalculated using the following relations

$$r_{film} = (1.0 - e^{(-kt)})r_{film} \tag{70}$$

$$r_{bulk} = (1.0 - e^{(-kt)})r_{bulk} \tag{71}$$

In Eqs. 70 and 71, the parameter k reduces the effect of the reaction at the beginning of the calculation. The default value of k is 1.0; however, the user can adjust the value manually. In our calculations typical values were between 1.0 and 0.01.

Starting from the point found as just described, the problem is integrated to the preset time $t + \Delta t$, and the independent variables are stored afterwards. The values obtained from the integration are used as a starting point for the Newton solver, which makes an attempt to solve the problem. If this attempt is successful, the program stops. In the case where the Newton solver fails, the program reads the solution from the previous integration, returns to the integrator, and continues the calculation. A loop counter controls whether a preset maximum number of relaxation/Newton iterations is reached.

Parameters that are important for the performance of the algorithm are mainly the inertia terms U^L and U^G, the integration time, Δt, and the maximum value for the loop counter. These parameters can be given manually, and it is fairly easy to find their corresponding values by trial and error.

When applying the hybrid method, it is especially important to set the maximum and minimum limitations for the variables during the Newton iteration to avoid the case where thermodynamic, physical property, mass transfer, and hydraulic models get physically impossible values of the variables for input, for example, negative flows or compositions. If the variables are not limited, the routines might fail, resulting in a run-time error of the program.

Simulation of Tray Hydrodynamics

Initialization of the variables for the Eddy-diffusion model

The set of second-order differential equations is very sensitive to the initial conditions. Thus it was difficult to achieve convergence from an arbitrary initial point. The initialization method used is based on the fact that it is possible to change the problem identically to the completely mixed liquid model by increasing the eddy diffusion coefficient to infinity.

Thus the problem is first solved using the normal rate-based model, the solution of this model being used as a starting point. Then, the problem is solved again, first with a very large value of the eddy-diffusion coefficient, and then gradually reducing it until the correct value is attained.

Simulation example with the Eddy-diffusion model

This model was used to simulate a pilot-scale reactive distillation column equipped with cross-flow reactive trays. The column studied is an MTBE-column in which the catalyst is assumed to be evenly distributed on the reactive trays in order to demonstrate the effect of the reaction on the tray profiles. The column arrangement is presented in Figure 6.

The strongly nonideal character of the mixture was taken into account. Altogether there were 20 trays in the column. In Figures 7 to 9, the simulated temperature and concentration profiles on the trays where the reaction takes place (in the column middle) are shown. Figure 7 represents the mixture temperature distribution, Figure 8 the concentrations of the reactant methanol, while Figure 9 shows the concentrations of the product MTBE. It is evident that the concentration changes are significant as compared to the difference between the individual stages. Nevertheless, the effect on the overall performance of the column is small. It seems that in this system with equilibrium limited reaction, different effects changing the tray concentration profiles reduce each other.

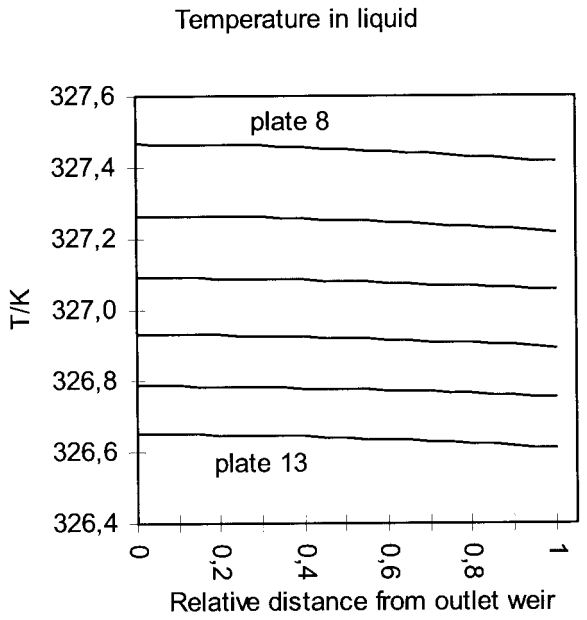

Figure 7. Liquid-temperature profiles on the reactive trays of a pilot-scale column according to the eddy-diffusion model.

Initialization of the variables for the mixed-pool model

Two methods for initialization of the variables were applied: the first method was to set the average feed composition at every pool on every tray. This is a straightforward method and works rather well with the usual distillation column models. However, rather long computation times are required, and therefore, it is advantageous to have initial values nearer to the solution. Alternatively, the problem was first solved using the traditional rate-based model, and then the mixed-pool model was initialized using the concentrations, temperatures, and flow rates of this solution.

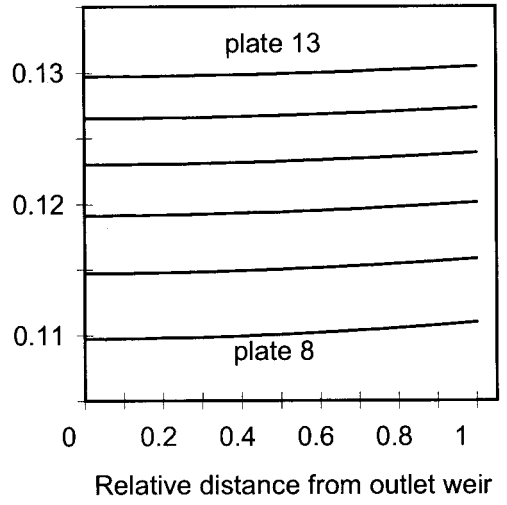

Figure 8. Liquid-phase concentration profiles of methanol on the reactive trays of a pilot-scale column according to the eddy-diffusion model.

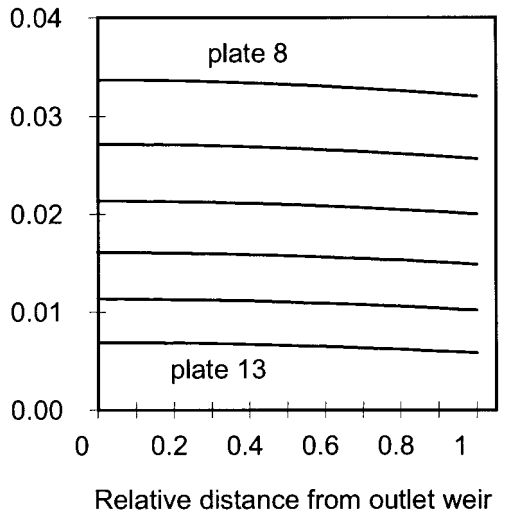

Figure 9. Liquid-phase concentration profiles of MTBE on the reactive trays of a pilot-scale column according to the eddy-diffusion model.

Simulation results with the mixed-pool model

The model has been applied to a system similar to that used with the eddy-diffusion model. In Figures 10 and 11 the calculated liquid-phase concentration profiles of the reactant methanol and reaction product MTBE are represented on the reactive trays of the column. The mass-transfer model for each pool is the mixed liquid–mixed vapor model.

Solving the example involving a column with 20 trays, 4 components, and 4 mixed pools on each tray was not difficult. However, the time penalty due to the large number of variables is apparent. The approximate time needed for one Newton step increased roughly proportional to the square of the numbers of the independent variables in the corresponding rate-based problem. The comments concerning the results achieved with the eddy-diffusion model apply to this case, too.

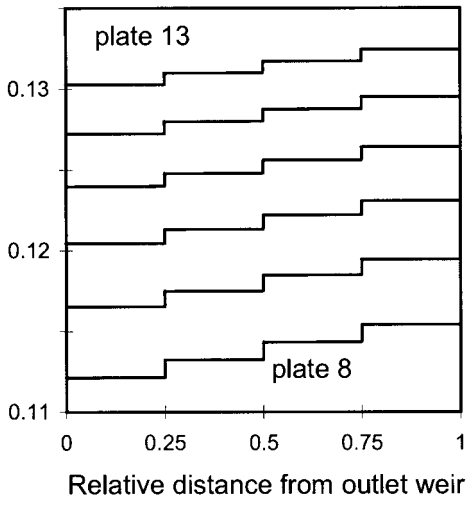

Figure 10. Liquid-phase concentration profiles of methanol on the reactive trays of a pilot-scale column according to the mixed-pool model.

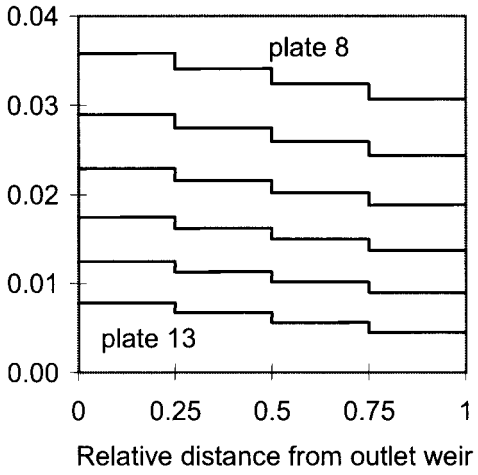

Figure 11. Liquid-phase concentration profiles of MTBE on the reactive trays of a pilot-scale column according to the mixed-pool model.

Experimental Validation of the Mass-Transfer Model in Macroporous Catalyst

The macroporous catalyst mass-transfer model presented in the section titled "Reaction and Mass Transfer in Macroporous Catalyst" can be validated by experimental data from Rehfinger and Hoffmann (1990b). These experimental data were obtained in a continuous stirred-tank reactor (CSTR). The investigated reaction was the liquid-phase synthesis of MTBE from methanol (MeOH) and isobutene (IB) with the commercial acidic ion-exchange resin Amberlyst 15 (Rohm & Haas) as catalyst. External mass-transfer resistance was experimentally excluded by a high stirrer speed. A narrow particle-size distribution of the applied catalyst was prepared by sieving the original catalyst.

The simulations were carried out based on the microkinetic model of Rehfinger and Hoffmann (1990a)

$$r = k_{\text{for}}(T)\left(\frac{a_{IB}}{a_{\text{MeOH}}} - \frac{1}{K_a}\frac{a_{MTBE}}{a_{\text{MeOH}}^2}\right), \tag{72}$$

with

$$k_{for}(T) = k_{\text{for}}(T^0)\exp\left[-\frac{E}{R_m}\left(\frac{1}{T}-\frac{1}{T^0}\right)\right]. \tag{73}$$

The kinetic parameters of the Arrhenius-equation (Eq. 73) are $k_{for}(T^0 = 333\text{ K}) = 15$ mmol/(s eq), $E = 92.4$ kJ/mol. The concentration of catalytically active sites of the used GPP-catalyst was $c_L = 0.9$ eq(H^+)/dm.

The multicomponent mass-transport phenomena were accounted for by calculating the catalyst effectiveness factor η from the numerical solution of the catalyst mass balances, as outlined earlier (see the section titled "Reaction and Mass Transfer in Macroporous Catalyst").

Figure 12 shows the comparison of experimental reaction rate data with simulation results for the commercial catalyst Amberlyst15. Furthermore, the simulated effectiveness factor and the intrinsic reaction rate (at bulk conditions) is depicted. The figure shows that the model predicts the experimental data quite well.

The reaction rate and the effectiveness factor increase strongly below a methanol concentration of about 0.5 mol/l. This ignition of the catalyst is due to the negative reaction order of the MTBE formation with respect to the reactant methanol (see Eq. 72).

Column Simulation Examples

The following numerical examples demonstrate the properties of the solution strategy. In these examples, a completely mixed liquid and a completely mixed vapor model are applied. Two chemical systems of interest have been chosen for the demonstration: the production of MTBE (etherification), and the production of methyl acetate (esterification). Altogether three column configurations are considered, two of which concern the MTBE production.

MTBE

According to the experience of the authors, Newton's method works well when the concentration of the MTBE in the product flow is low. However, finding the solution for the higher MTBE product level often requires tedious nursing of the solution. Experience with the MTBE case simulation using Newton's method also can be found in (Zheng and Xu, 1992).

An example column used here has a catalyst section in the middle, a stripping section, and a rectifying one. The catalyst section is filled with glass-supported acidic polymer catalyst (GPP catalyst (Kunz, 1998)). The MeOH feed is introduced just above and the hydrocarbon feed just below the catalyst section. The rest of the column consists of random packed beds. The hydrodynamic model applied was the mixed liquid–mixed vapor model. The kinetic model was taken from Rehfinger and Hoffmann (1990a,b), as were the UNIQUAC interaction parameters for the VLE calculation. The binary diffusivities were calculated in the liquid phase with the method of Tyn and Calus and in the vapor phase with the method of Fuller (see, for example, Reid et al. (1987)). The

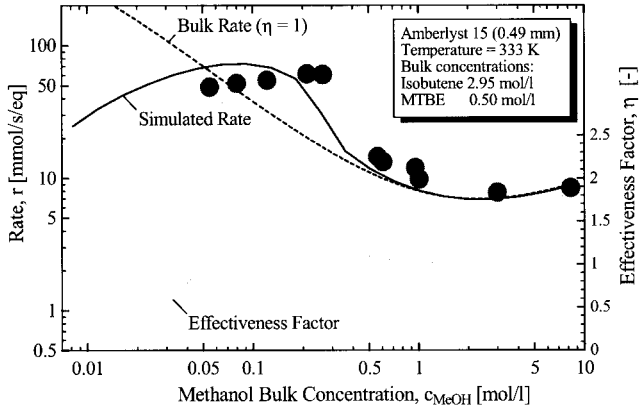

Figure 12. Experimental and simulated reaction rate *r* and effectiveness factor η of the MTBE synthesis vs. the bulk-phase methanol concentration (experimental data from Rehfinger and Hoffmann, 1990b).

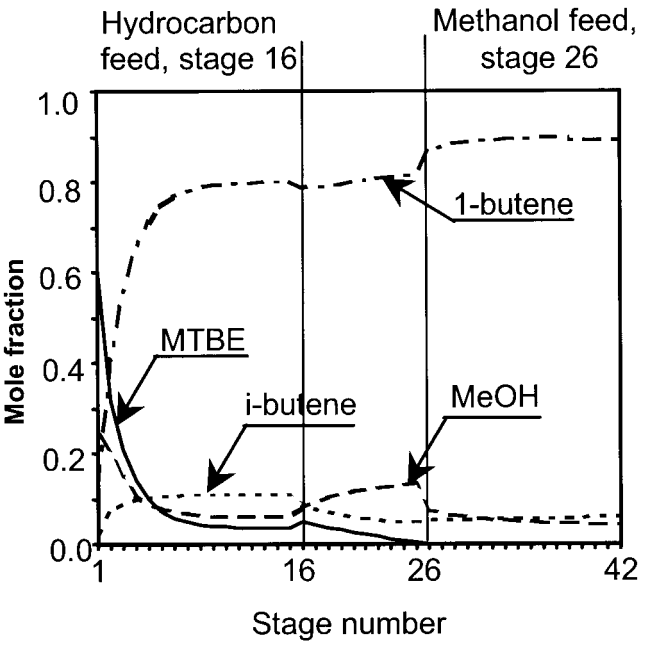

Figure 13. Simulation of MTBE synthesis with low reboiler concentration of MTBE, liquid composition profiles; catalytic stages are 17–26.

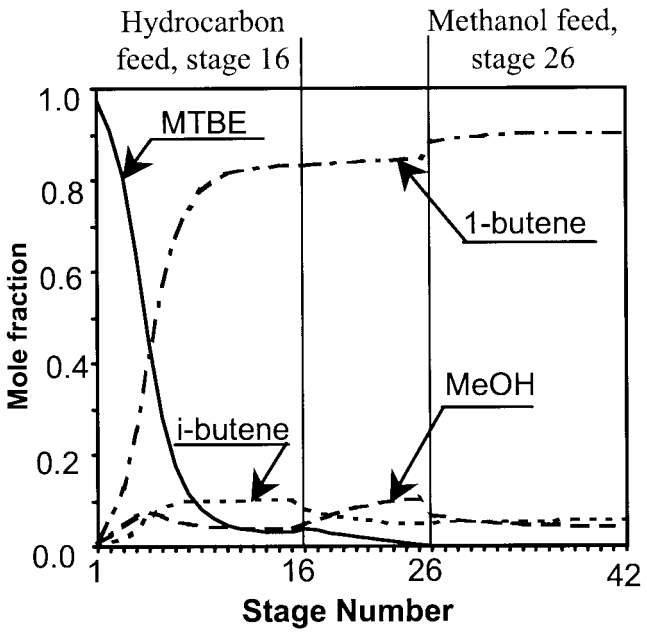

Figure 14. Simulation of MTBE synthesis with high reboiler concentration of MTBE, liquid composition profiles; catalytic stages are 17–26.

vapor and liquid binary mass-transfer correlations were calculated for the inert packing and the GPP rings with the correlation of Onda et al. (1968).

A number of additional physical properties are taken from DIPPR correlations or from methods presented in Reid et al. (1987). The initial number of stages was determined assuming the height of a stage to be approximately equal to one-third of the height equivalent to a theoretical plate (HETP) value.

When the Newton solver was used independently, the solution was found easily for the simulation with low composition of MTBE in the product flow. This took about 10 Jacobian matrix evaluations. The liquid composition profile of this simulation is shown in Figure 13. On the other hand, the simulations resulting in a high MTBE composition in the product did not converge with the Newton's method alone. However, with an integration over 15 s (model time) and small inertia terms on the segments, the relaxation method was able to deliver a good starting point for Newton's method (see Table 1 for computational details), and the problem could be solved. Figure 14 demonstrates the liquid composition profiles for this simulation.

Methyl acetate

The methyl acetate example is extracted from Agreda et al. (1990), who present typical composition and temperature profiles for a pilot-scale column. The specification of this column is completed by some engineering estimates and in-house NRTL parameters for VLE computations and for the kinetic model parameters. The impurities reported by Agreda et al. (1990) are not included in our simulation. An attempt to solve this problem with Newton's method alone failed, and it is worthy of note that Agreda et al. also reported convergence difficulties when using a Newton-based method. On the other hand, the hybrid method found the solution readily (see Table 1). The composition profiles obtained with this method are shown in Figure 15.

Comparison with Experimental Results

DESIGNER has been tested against experimental results gathered from the reactive distillation test runs carried out by the project partners at pilot and laboratory scale. The reactive distillation column used as an example here had a catalytic section in the middle part of the column. The total height of the column is 12 m and the diameter of the column is 0.16 m. This catalytic section consists either of a packed bed of catalytically active rings (see Sundmacher and Hoffmann (1996)) or of the new structured catalytic packing that has been developed in this project (Górak et al., 1998). The rectifying and stripping parts consist of two separately supported packing sections and are

Table 1. Hybrid Solver Performance for the Cases Considered

	Hybrid Solver			
	Relaxation Method		Newton's Method	
Case	Integration Time (s)	Residual Function Calls	Jacobian Matrix Evaluations	Total CPU Time (s)
MTBE, high reboiler concentration	15	2129	7	690
Methyl acetate	20	2908	8	2310

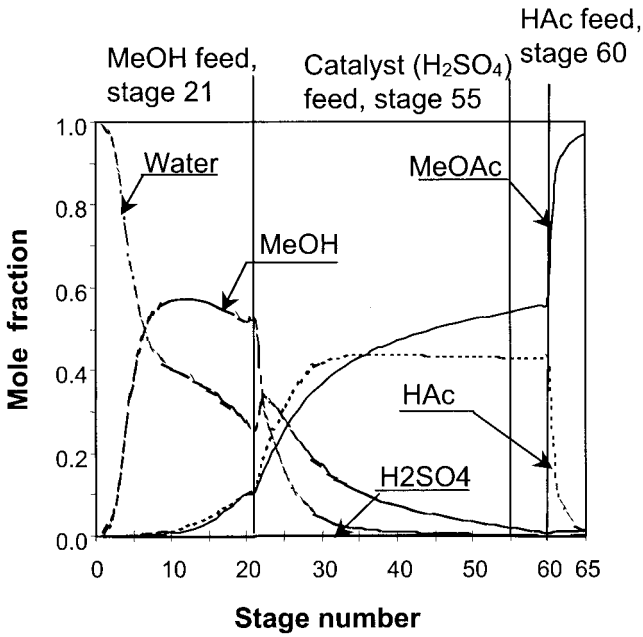

Figure 15. Simulation of methyl acetate synthesis, liquid composition profiles.

filled with Intalox Metal Tower Packing. The methanol feed was introduced just above and the hydrocarbon feed just below the catalyst section of the column.

Due to the diameter of the column (0.16 m), in these simulations the completely mixed liquid and completely mixed vapor model was used. The results of simulation of an experiment with the catalytic rings were presented earlier by Kenig et al. (1999). In the simulations, four components, namely, methanol, isobutene, MTBE, and 1-butene, were chosen to describe the system under consideration. The simulated results agree well with experimental values. Similar simulations were performed by Sundmacher and Hoffmann (1996) for a significantly smaller column.

A further case study concerns the column with the structured catalytic packing Multipak®. The column structure is similar to that just described, except that the catalyst section is equipped with catalytic structured packing. The chemical system used involves 11 components, namely methanol, isobutene, *i*-butane, *n*-butane, propane, 1-butene, *trans*-2-butene, *cis*-2-butene, isopentane, *n*-pentane, MTBE. The catalyst section in the column contained totally 3.6–4.0 kg of dry Amberlyst 15 ion-exchange resin. Altogether 11 test runs were performed. The pressure of the column varied between 800 and 1000 kPa, and the reflux ratio between 2 and 3. The molar ratio methanol/isobutene varied between 1.27 and 1.41.

In the simulations, VLE is calculated by the Wilson method. The parameters used are in-house parameters of Fortum Oyj. Typical composition profiles in the liquid bulk for one experiment were shown in (Kenig et al., 1999), with good agreement between calculated and measured values.

A comparison of experimental and simulated results is performed here for all 11 test runs. Generally, good agreement between the calculated and experimental conversion of isobutene can be established, with an average deviation of less than 5% (Figure 16). The model is also able to predict well the distillate compositions (Figure 17).

Figure 18 summarizes the simulated and experimental liquid bottoms product concentrations of MTBE for all 11 test runs. The reaction rates seem to be slightly underestimated, which leads to deviations between the simulated and experimental values.

These case studies were performed with Newton's method. Although convergence was good, the computations with the rate-based model usually took 50 to 60 times longer than with the ideal-stage model used as the reference. This is explained both by a larger set of independent variables and equations and by the need of using more stages in the rate-based model.

Another successful test of DESIGNER was accomplished with the ethyl acetate synthesis from acetic acid and ethanol (Kenig et al., 2001).

Conclusions

In this article, a computer-aided tool, DESIGNER, for the simulation of reactive distillation columns is presented. DESIGNER constitutes a completely rate-based simulator for steady-state reactive distillation operations developed in the context of the three-year BRITE-EURAM project "Reactive distillation" supported by the EU.

The model development of DESIGNER is detailed, the structural and numerical peculiarities are discussed, and a number of simulation examples are presented that illustrate the properties of the simulator.

DESIGNER comprises several model libraries containing particular models for material and energy balances, vapor–liquid equilibrium, mass transfer and hydrodynamics, reaction kinetics, and so forth.

The structure is based on a discretized representation of the reactive distillation unit and is general enough to provide a modeling basis for various process configurations suitable for reactive distillation.

The aspects of particular interest for the DESIGNER devel-

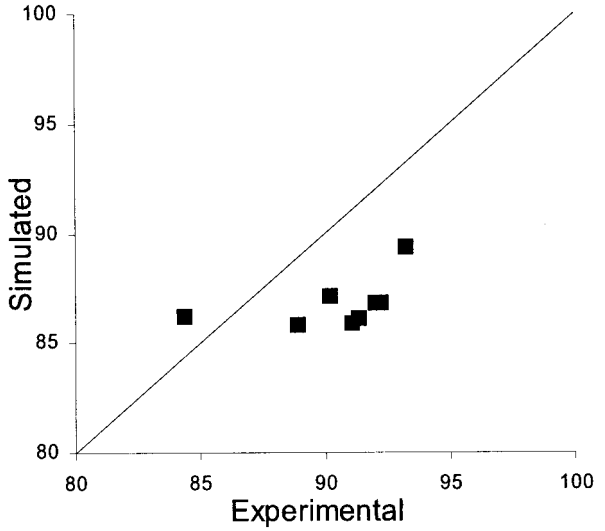

Figure 16. Experimental and simulated conversion of isobutene (all 11 test runs) for the column with the reactive section filled with catalytic structured packing Multipak®.

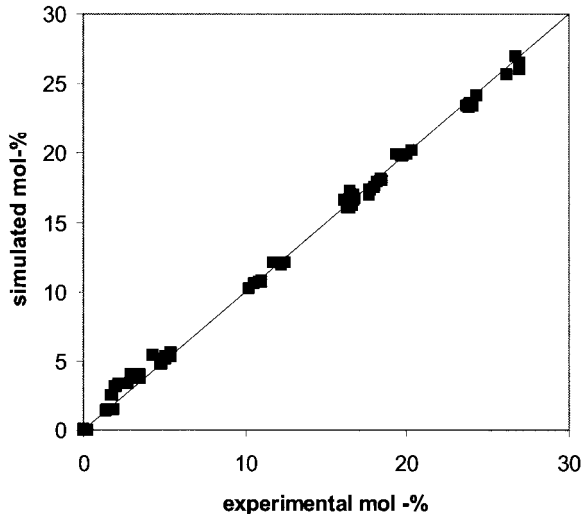

Figure 17. Experimental and simulated liquid distillate compositions (all 11 test runs) for the column with the reactive section filled with catalytic structured packing Multipak™.

opment were a mass-transfer model, including the reaction in the film region, a catalyst efficiency determination based on the mass transfer inside the catalyst, and the hydrodynamic models for reactive trays. These aspects are discussed at length in this article.

To ensure a reliable solution of the resulting complex nonlinear systems of equations, a special solver development was accomplished. The Newton method alone usually requires application of a sequence of models with increasing complexity: equilibrium, rate-based without reaction, rate-based with slow reaction, rate-based with real reaction. To enhance the convergence, a hybrid solver was developed that combines the relaxation method with Newton's approach. Numerous simulation examples representing typical reactive distillation problems demonstrated that the hybrid solver clearly extend the domain of convergence as compared with the Newton solver. The computational times of the hybrid method are acceptable, since it is often sufficient to make only one step toward the desired solution. The results thus found can be used as a starting point for the subsequent simulations using Newton's method.

Two tray-scale rate-based hydrodynamic models, that is, the eddy-diffusion model and mixed-pool model for reactive cross-flow trays, have been developed and implemented in DESIGNER. These models are valuable when the plates are large and the Murphree efficiency might exceed 1.0 (e.g., large reactive cross-flow trays) or when the concentration gradients on the plate significantly influence the reaction rate.

The simulated examples demonstrated that liquid concentrations vary considerably over a distillation tray and this variation should be taken into account in a rigorous model. The increased complexity of the models and the resulting long computation time is an obvious disadvantage. In their current state the models are not likely to be used in everyday simulations, but, for example, they can be applied for checking the mass transfer and hydraulic performance, and thus be helpful for final design of certain critical columns. The application of these models may be, for instance, valuable for large-diameter tray absorbers with highly exothermal reactions.

It has turned out that the mass-transport phenomena inside the catalyst can play a major role for the performance of a catalytic distillation column. In particular, fast chemical reactions are affected by internal mass-transport limitations. Since in reactive distillation processes, the reaction temperature is dependent on the total operating pressure, catalyst mass-transport limitations are of major significance at elevated column pressures (see also Mohl et al. (2001)). In such a case, the component mass balances at the catalyst have to be solved simultaneously along with the equations for the column stages, which results in a large-scale differential–algebraic system. DESIGNER handles this problem by using the catalyst effectiveness factor, which is continuously calculated from the catalyst mass balances.

DESIGNER has been evaluated and improved in the project by universities and industrial partners using several model and real case studies. Both the models and numerical methods developed demonstrate good abilities when simulating complex reactive distillation operations. In the present article, simulation examples are given for methyl acetate synthesis and the MTBE system. Investigation of a similar system, ethyl acetate synthesis by reactive distillation, has been published recently by Kenig et al. (2001).

The main advantages of DESIGNER are the direct account of mass and heat transport (rate-based approach), multicomponent mass-transport description via the Maxwell-Stefan equations, consideration of a large spectrum of reactions (homogeneous and heterogeneous; slow, average and fast; equilibrium and kinetically controlled), reaction account in both bulk and film phases, availability of different hydrodynamic models, and a large choice of hydrodynamic and mass-transfer correlations for various types of column (trays, random and structured packings, catalytic packings).

In addition, DESIGNER's flexibility and open character allow easy adaptation to various column configurations and process conditions.

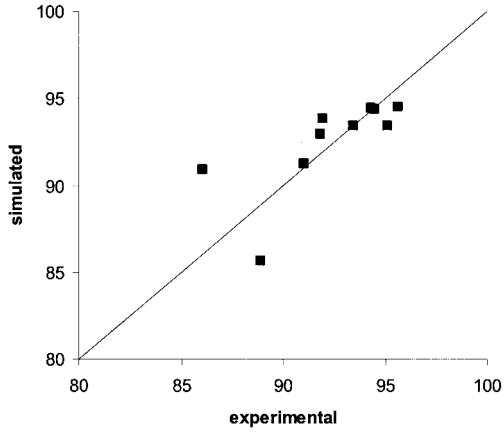

Figure 18. Experimental and simulated liquid bottoms product concentrations of MTBE (all 11 test runs) for the column with the reactive section filled with catalytic structured packing Multipak®.

Acknowledgment

The support by the European Commission in the frame of the BRITE-EURAM program (CEC Project No. BE95-1335) is greatly acknowledged.

Notation

a_i = activity of species i
a^I = specific gas–liquid interfacial area, m^2/m^3
A = geometry shape parameter (slab: $A = 0$, cylinder: $A = 1$, sphere: $A = 2$)
A_c = column cross section, m^2
A_R = affinity of chemical reaction, J/mol
c_i = molar concentration of species i, mol/m^3
c_L = mean acid group concentration in Eq. 52, (Eq. H^+)/m^3
c_t = liquid mixture molar density, mol/m^3
$\tilde{\mathbf{c}}$ = column vector consisting of c_i, dimension n, mol/m^3
C = coefficient defined by $C = 1/(h_f c_t D_e w)$
$Đ_{ij}$ = Maxwell-Stefan diffusivity of binary pair $i - j$, m^2/s
D_e = eddy diffusion coefficient, m^2/s
$[D]$ = matrix of multicomponent diffusion coefficients, m^2/s
E'_k = heat transfer rate on tray k per unit length of flow path, J/(m s)
E = activation energy, J/mol
$\mathbf{f}_m$ = vector of residual functions of the stage model
$F^G_{i,k}$, $F^L_{i,k}$ = vapor and liquid feeds of component i to tray k, mol/s
G = vapor molar flow rate, mol/s
G'_k = vapor molar flow rate from tray k per unit length of flow path, mol/(m s)
h_f = froth height, m
h_k = liquid enthalpy on tray k, J/mol
H_k = vapor enthalpy on tray k, J/mol,
J_i = molar diffusion flux of species i, $mol/(m^2 s)$
$\mathbf{J}$ = vector consisting of J_i, $mol/(m^2 s)$
$[J_m]$ = Jacobian matrix
k = parameter of Eqs. 70 and 71
k_{for} = reaction rate constant of forward reaction
k_{rev} = reaction rate constant of reverse reaction
$\tilde{\mathbf{k}}^T$ = column vector consisting of reaction velocity constants, dimension n, $mol/(m^3 s)$
K_i = phase-distribution coefficient
K_a = chemical-equilibrium constant based on activities
K_i^{eq} = equilibrium constant of reaction i
$[K]$, $[\hat{K}]$ = reduced reaction kinetic matrices, dimension $(n - 1)$, 1/s
$[\tilde{K}]$ = reaction kinetic matrix, dimension n, 1/s
l = flow coordinate in eddy-diffusion model directed from outlet to inlet weir, m
l_a = axial coordinate directed from column top to bottom, m
l_f = total length of the flow path (distance between inlet and outlet weirs), m
L = liquid molar flow rate, mol/s
L_p = characteristic length of the catalytic pellet, m
m = number of reactions
m_i = reaction order associated with species i
MTR = total mass-transfer resistance in catalyst, s/m^2
n = number of components of mixture
N_i = molar flux of species i, $mol/(m^2 s)$
$N'_{i,k}$ = mass-transfer rate of component i on tray k per unit length of flow path, mol/(m s)
$N^{calc}_{i,k}$ = calculated mass-transfer rate per unit length on tray k, mol/(m s)
$\mathbf{N}_r$ = vector of mass-transfer rates, mol/s
p_k = pressure on tray k, Pa
Δp_k^{spec} = specified pressure drop on tray k, Pa
r = volumetric reaction rate, $mol/(m^3 s)$
$R'_{i,k}$ = reaction rate of component i on tray k per unit length of flow path, mol/(m s)
R_g = gas constant, 8.3144 J/mol K
$\tilde{\mathbf{R}}$ = vector consisting of chemical production rates, dimension n, $mol/(m^3 s)$
$\mathbf{R}$ = reduced vector consisting of chemical production rates, dimension $(n - 1)$, $mol/(m^3 s)$
s = damping factor
S_k = side draw, mol/s
t = time, s
T = temperature, K
u = number of mixed pools on a stage
U = specific molar holdup, mol/m
w = width of the liquid flow path, m
x_i = liquid mole fraction of species i
$\mathbf{x}$ = reduced vector consisting of x_i, dimension $(n - 1)$
$\tilde{\mathbf{x}}$ = vector consisting of x_i, dimension n
$\mathbf{X}_m$ = vector of independent variables of a reactive distillation stage
y_i = vapor mole fraction of species i
$\mathbf{y}$ = reduced vector consisting of y_i, dimension $(n - 1)$
$y^*_{i,k}$ = vapor mole fraction of species i on tray k at equilibrium with bulk liquid
z = coordinate, m
z_p = radial coordinate directed from the center of the catalytic pellet to the surface, m
z_f = film coordinate directed from the gas phase to the liquid phase, m

Greek letters

α = reaction affinity ratio
δ = effective film thickness, m
ε_p = void fraction of catalyst
η = effectiveness factor
λ = enhancement factor
μ_i = chemical potential of species i, J/mol
ν_i = stoichiometric coefficient of species i in an arbitrary reaction
ρ = dimensionless rate of reaction (Eq. 58)
ϕ_L = volumetric liquid holdup, m^3/m^3
ϕ = Thiele modulus
τ = tortuosity factor of catalyst
ξ = dimensionless film coordinate
$\zeta = z_p/L_p$ = dimensionless coordinate

Subscripts and Superscripts

G = vapor phase
i, j = component indices
k = stage (tray) index
L = liquid phase
t = total
B = bulk phase
f = liquid film
F = feed flow
I = phase interface
T = transpose
L = liquid phase
G = vapor phase
$\sim$ = indicates dimension n if necessary to discriminate from dimension $(n - 1)$

Literature Cited

Agreda, V. H., L. R. Partin, and W. H. Heise, "High-Purity Methyl Acetate via Reactive Distillation," *Chem. Eng. Prog.,* **86**(2), 40 (1990).

Alejski, K., "Computation of the Reacting Distillation Column Using a Liquid Mixing Model on the Plates," *Comput. Chem. Eng.,* **15,** 313 (1991).

Ashley, M. J., and G. G. Haselden, "The Calculation of Plate Efficiency Under Conditions of Finite Mixing in Both Phases in Multiplate Columns, and the Potential Advantage of Parallel Flow," *Chem. Eng. Sci.,* **25,** 1665 (1970).

Astarita, G., and S. I. Sandler, eds., *Kinetic and Thermodynamic Lumping of Multicomponent Mixtures,* Elsevier, Amsterdam, The Netherlands (1991).

Danckwerts, P. V., *Gas-Liquid Reactions,* McGraw-Hill, New York (1970).

DeGarmo, J. L., V. N. Parulekar, and V. Pinjala, "Consider Reactive Distillation," *Chem. Eng. Prog.,* **88**(3), 43 (1992).

DeLancey, G. B., "Multicomponent Film-Penetration Theory with Linearized Kinetics—I. Linearization Theory and Flux Expressions," *Chem. Eng. Sci.,* **29,** 2315 (1974).

Doherty, M. F., and G. Buzad, "Reactive Distillation by Design," *Trans. Inst. Chem. Eng.,* **70**(Part A), 448 (1992).

Doraiswamy, L. L., and M. M. Sharma, *Heterogeneous Reactions: Analysis, Examples and Reactor Design,* Wiley, New York (1984).
Fieg, G., W. Gutermuth, W. Kothe, H.-H. Mayer, S. Nagel, H. Wendeler, and G. Wozny, "A Standard Interface for Use of Thermodynamics in Process Simulation," *Comput. Chem. Eng.,* **19,** S317 (1995).
Gerster, J. A., A. B. Hill, N. N. Hochgraf, and D. G. Robinson, *Tray Efficiencies in Distillation Columns,* AIChE, New York (1958).
Górak, A., "Simulation thermischer Trennverfahren fluider Vielkomponentengemische," *Prozeßsimulation,* H. Schuler, ed., Verlag Chemie, Weinheim, Germany (1995).
Górak, A., L. U. Kreul, and M. Skowronski, Patent Pending DE 197 01 045 A1, Germany (1998).
Henley, E. J., and J. D. Seader, *Equilibrium Stage Separation Operations in Chemical Engineering,* Wiley, New York (1981).
Higler, A., R. Krishna, and R. Taylor, "Nonequilibrium Cell Model for Multicomponent (Reactive) Separation Processes," *AIChE J.,* **45,** 2357 (1999).
Hikita, H., and S. Asai, "Gas Asorption with (m, n)-th Order Irreversible Chemical Reaction," *Int. Chem. Eng.,* **4,** 332 (1964).
Hirschfelder, J. O., C. F. Curtiss, and R. B. Bird, *Molecular Theory of Gases and Liquids,* Wiley, New York (1964).
Katti, S. S., "Gas-Liquid Solid Systems: An Industrial Perspective," *Trans. Inst. Chem. Eng.,* **73**(Part A), 595 (1995).
Kenig, E. Y., and L. P. Kholpanov, "Analysis of Formulation and Solution of Multicomponent Reaction-Diffusion Problems," *Theor. Found. Chem. Eng.,* **26,** 510 (1992).
Kenig, E. Y., L. P. Kholpanov, and V. A. Malyusov, "Mathematical Model and Calculation Method for Multicomponent Combined Reaction-Diffusion Processes in Column Apparatuses," *Proc. Acad. Sci. USSR, Chem. Technol. Sec.,* **324,** 55 (1992).
Kenig, E. Y., and A. Górak, "A Film Model Based Approach for Simulation of Multicomponent Reactive Separation," *Chem. Eng. Process.,* **34,** 97 (1995).
Kenig, E. Y., K. Jakobsson, P. Banik, J. Aittamaa, A. Górak, M. Koskinen, and P. Wettmann, "An Integrated Tool for Synthesis and Design of Reactive Distillation," *Chem. Eng. Sci.,* **54,** 1347 (1999).
Kenig, E. Y., F. Butzmann, L. Kucka, and A. Górak, "Comparison of Numerical and Analytical Solutions of a Multicomponent Reaction-Mass-Transfer Problem in Terms of the Film Model," *Chem. Eng. Sci.,* **55,** 1483 (2000).
Kenig, E. Y., H. Bäder, A. Górak, B. Bessling, T. Adrian, and H. Schoenmakers, "Investigation of Ethyl Acetate Reactive Distillation Process," *Chem. Eng. Sci.,* **56,** 6185 (2001).
King, C. J., *Separation Processes,* McGraw-Hill, New York (1980).
Kister, H. Z., *Distillation Design,* McGraw-Hill, New York (1992).
Kooijman, H. A., and R. Taylor, "Modeling Mass Transfer in Multicomponent Distillation," *Chem. Eng. J.,* **57,** 177 (1995).
Kunz, U., "Entwicklung neuartiger Polymer/Träger-Ionenaustauscher als Katalysatoren für chemische Reaktionen in Füllkörperkolonnen," Habilitation, Tech. Univ. of Clausthal, Clausthal-Zellerfeld, Germany (1998).
Kunz, U., and U. Hoffmann, "Preparation of Catalytic Polymer/Ceramic Ionexchange Packings for Reaction Distillation Columns," *Preparation of Catalyst VI,* G Poncelet et al., ed., Elsevier Science BV, Amsterdam, The Netherlands (1995).
Lewis, W. K., and W. G. Whitman, "Principles of Gas Absorption," *Ind. Eng. Chem.,* **16,** 1215 (1924).
Lockett, M. J., *Distillation Tray Fundamentals,* Elsevier, Amsterdam, The Netherlands (1991).
Mackowiak, J., *Fluiddynamik in Kolonnen mit modernen Füllkörperpackungen und Packungen für Gas/Flüssigkeitssysteme,* Sauerländer, Frankfurt am Main, Germany (1991).
Malone, M. F., and M. F. Doherty, "Reactive Distillation," *Ind. Eng. Chem. Res.,* **39,** 3953 (2000).
Mohl, K. D., A. Kienle, K. Sundmacher, and E. D. Gilles, "A Theoretical Study of Kinetic Instabilities in Catalytic Distillation Processes: Influence of Transport Limitations Inside the Catalyst," *Chem. Eng. Sci.,* **56,** 5239 (2001).
Noeres, C., E. Y. Kenig, and A. Górak, "Modelling of Reactive Separation Processes: Reactive Absorption and Reactive Distillation," *Chem. Eng. Process.,* **42,** 157 (2003).
Onda, K., Takeuchi, H., and Y. Okumoto, "Mass Transfer Coefficients Between Gas and Liquid Phases in Packed Columns," *J. Chem. Eng. Jpn.,* **1,** 56 (1968).
Patankar, S. V., *Numerical Heat Transfer and Fluid Flow,* Hemisphere, McGraw-Hill, New York (1980).
Rehfinger, A., and U. Hoffmann, "Kinetics of Methyl Tertiary Butyl Ether Liquid Phase Synthesis Catalyzed by Ion Exchange Resin—I. Intrinsic Rate Expression in Liquid Phase Activities," *Chem. Eng. Sci.,* **45,** 1605 (1990a).
Rehfinger, A., and U. Hoffmann, "Kinetics of Methyl Tertiary Butyl Ether Liquid Phase Synthesis Catalyzed by Ion Exchange Resin—II. Macropore Diffusion of MeOH as Rate-Controlling Step," *Chem. Eng. Sci.,* **45,** 1619 (1990b).
Reid, R. C., J. M. Prausnitz, and B. E. Poling, *The Properties of Gases and Liquids,* McGraw-Hill, New York (1987).
Rocha, J. A., J. L. Bravo, and J. R. Fair, "Distillation Columns Containing Structured Packings—1. Hydraulic Models," *Ind. Eng. Chem. Res.,* **32,** 641 (1993).
Sakuth, M., D. Reusch, and R. Janowsky, "Reactive Distillation," *Ullmann's Encyclopedia of Industrial Chemistry,* Wiley-VCH, Weinheim, Germany (2001).
Seader, J. D., "The Rate-Based Approach for Modeling Staged Separations," *Chem. Eng. Prog.,* **85**(10), 41 (1989).
Sherwood, T. K., R. L. Pigford, and C. R. Wilke, *Mass Transfer,* McGraw-Hill, New York (1975).
Stewart, W. E., and R. Prober, "Matrix Calculation of Multicomponent Mass Transfer in Isothermal Systems," *Ind. Eng. Chem. Fundam.,* **3,** 224 (1964).
Stichlmair, J., J. L. Bravo, and J. R. Fair, "General Model for Prediction of Pressure Drop and Capacity of Countercurrent Gas/Liquid Packed Columns," *Gas Sep. Purif.,* **3,** 19 (1989).
Sundmacher, K., L. K. Rihko, and U. Hoffmann, "Classification of Reactive Distillation Processes by Dimensionless Numbers," *Chem. Eng. Commun.,* **127,** 151 (1994).
Sundmacher, K., and U. Hoffmann, "Development of a New Catalytic Distillation Process for Fuel Ethers via a Detailed Nonequilibrium Model," *Chem. Eng. Sci.,* **51,** 2359 (1996).
Taylor, R., and R. Krishna, *Multicomponent Mass Transfer,* Wiley, New York (1993).
Taylor, R., and R. Krishna, "Modelling Reactive Distillation," *Chem. Eng. Sci.,* **55,** 5183 (2000).
Taylor, R., H. A. Kooijman, and J.-S. Hung, "A 2nd Generation Nonequilibrium Model for Computer-Simulation of Multicomponent Separation Processes," *Comput. Chem. Eng.,* **18,** 205 (1994).
Toor, H. L., "Solution of the Linearized Equations of Multicomponent Mass Transfer," *AIChE J.,* **10,** 448, 460 (1964a).
Toor, H. L., "Prediction of Efficiencies and Mass Transfer on a Stage with Multicomponent Systems," *AIChE J.,* **10,** 545 (1964b).
Toor, H. L., "Dual Diffusion—Reaction Coupling in First Order Multicomponent Systems," *Chem. Eng. Sci.,* **20,** 941 (1965).
Towler, G. P., and S. J. Frey, "Reactive Distillation," *Reactive Separation Processes,* S. Kulprathipanja, ed., Taylor & Francis, Philadelphia (2001).
Treybal, R. E., *Mass-Transfer Operations,* McGraw-Hill, New York, 1980.
Wei, J., and C. D. Prater, "The Structure and Analysis of Complex Reaction Systems," *Adv. Catal.,* **13,** 203 (1962).
Wesselingh, H., and R. Krishna, *Mass Transfer in Multicomponent Mixtures,* Delft Univ. Press, Delft, The Netherlands (2000).
Wheeler, A., "Reaction Rates and Selectivity in Catalyst Pores," *Adv. Catal.,* **3,** 250 (1951).
Wörz, O., and H.-H. Mayer, "Reaction Columns," *Ullmann's Encyclopedia of Industrial Chemistry,* Wiley-VCH, Weinheim, Germany (2001).
Zheng, Y., and X. Xu, "Study on Catalytic Distillation Process. Part II. Simulation of Catalytic Distillation Process," *Trans. Inst. Chem. Eng.,* **70** (Part A), 465 (1992).
Zogg, M., *Wärme- und Stofftransportprozesse,* Otto Salle Verlag, Frankfurt am Main, and Verlag Sauerländer, Aarau, Germany (1983).

Manuscript received Sept. 17, 2002, and revision received June 16, 2003.